Title
Evaluation Of Radio Links And Networks

Authors
Linnartz, Jean-paul M. G.
Diesta, Rolando F.

Publication Date
1996

CALIFORNIA PATH PROGRAM
INSTITUTE OF TRANSPORTATION STUDIES
UNIVERSITY OF CALIFORNIA, BERKELEY

Evaluation of Radio Links and Networks

Jean-Paul M.G. Linnartz
Rolando F. Diesta

California PATH Research Report
UCB-ITS-PRR-96-16

This work was performed as part of the California PATH Program of the University of California, in cooperation with the State of California Business, Transportation, and Housing Agency, Department of Transportation; and the United States Department of Transportation, Federal Highway Administration.

June 1996

ISSN 1055-1425

EVALUATION OF RADIO LINKS

AND NETWORKS

TABLE OF CONTENTS

Chapter 1

Introduction

1.1 Introduction

Advanced technology may mitigate some of the existing ground transportation problems, such as traffic congestion. Projects such as Road Automobile Communication Systems (RACS) in Japan [1], PROMETHEUS in Europe [2], and Partners for Advanced Transit and Highway (PATH) in the U.S. are currently engaged in the design of such systems called Intelligent Transportation Systems (ITS) in Japan and the United States and Road Transport Informatics (RTI) in Europe. These projects develop methods and techniques to improve safety and efficiency of the highway system, which in turn would lead to an increase in the productivity of commuters as well as alleviate pollution [3]. Mobile-to-mobile communication is of critical importance to such ITS projects, especially in Automated Vehicle Control Systems (AVCS) employing platoons [4].

This study was motivated by research on AVCS, in which vehicles periodically exchange telemetric data, for instance on their speed and acceleration. This allows smooth control of vehicles speeds without the effects of small acceleration errors in the control loop

propagating backwards and being amplified in the reactions of following vehicles. Communication could be achieved through roadside base stations, but the frequency reuse can be denser and the system may be more economical if direct car-to-car links are used. Both radio and infrared are considered as an option for communication between cars within a platoon while (leaders of) platoons always communicate over longer ranges where radio may be preferred. Platoons may communicate through base stations, as their messages mostly need to be monitored and processed by a landbased system entity anyhow. Although communication occurs only over relatively short range, on the order of tens of meters, the communication links have to be extremely reliable. Earlier PATH studies showed that reliable operation of such systems requires updates to arrives at least once every 50 millisecond for communication within a platoon and somewhat more lenient requirements for communication between platoons. Communication channel fades exceeding this duration will severely affect the reliabilty of the radio link.

In our research, we relied heavily upon statistical models. For instance the radio propagation channel is regarded to consist of a large set of reflected waves, however with a few dominant and components and many small random omponents. In this respect, we address certain aspects already brought forward in the report by Polydoros and others at University of Southern California [5]. Their conclusion appeared to be that the phasor addition of reflected waves may cause destructive cancellation in certain areas, which makes the radio links less reliably if vehicles are in particular locations. While USC researchers considered a certain (discrete) number of relevant components, we modelled two main contributing components (the line-of-sight and the ground-reflected path), plus a large, possibly infinite number of weak reflections. These reflection were not treated deterministically, but are cvonsidered as random variables.

This report also documents measurements of the vehicle-to-vehicle link. While a vast amount of propagation data is available in open literature for cellular communications, the peculiarities of the car to car channel received little attention..

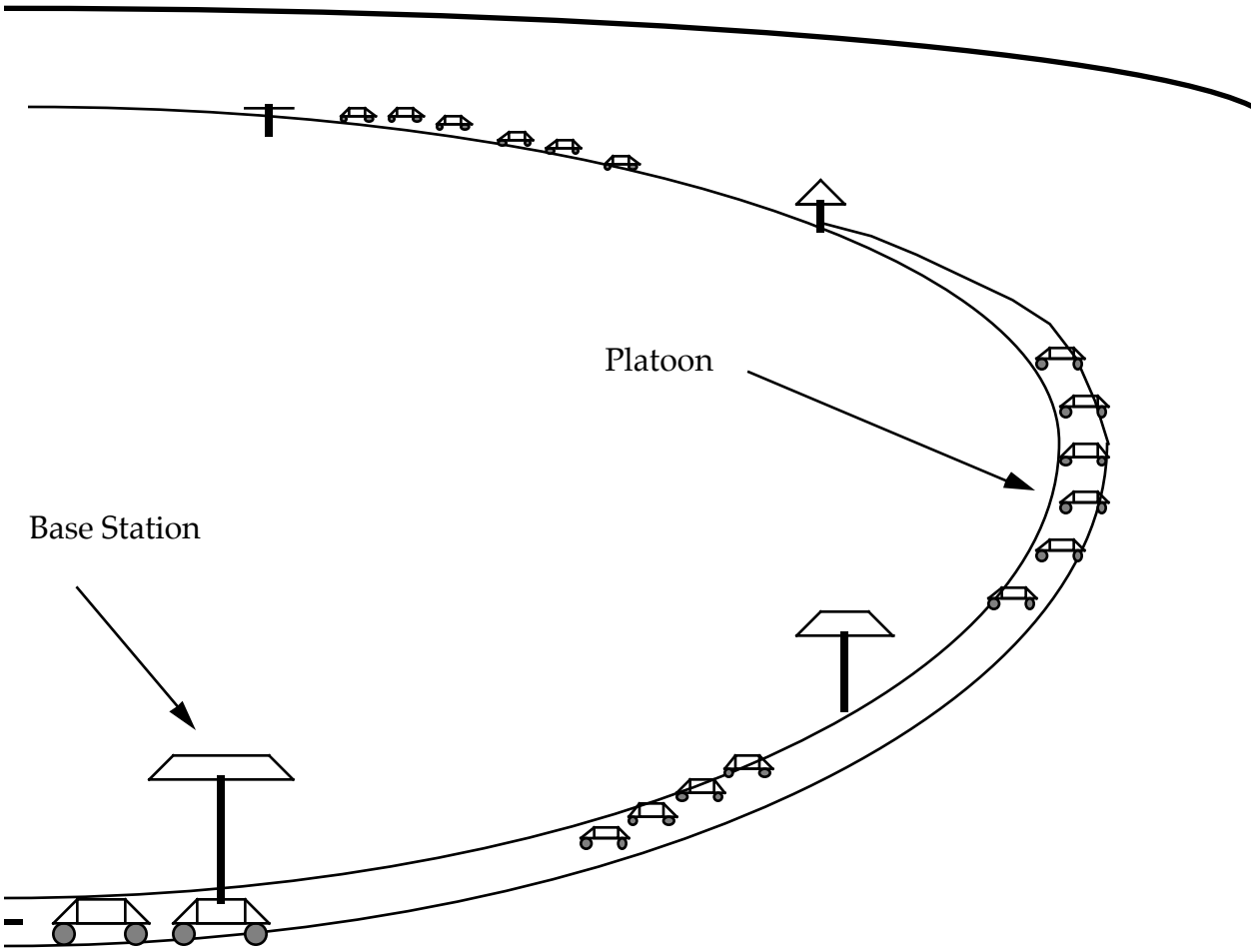

Figure 1.1 *The ITS communication scenario.*

The performance of the radio link is evaluated for various modulation methods. In particular we compare TDMA transmission schemes with spread-spectrum methods, such as Direct Sequence and Frequency Hopping. As can be understood intuitively, the performance of the system increases with the spread-factor applied. Large spread factors however imply that more bandwidth is used. When systems are compared on an equal bandwidth base, uspread (TDMA) systems typically allow very frequent updates of vehicle data. While each transmission is relatively vulnerable to interference, the probability of receiving at least one message within the deadline rerquirements typically is larger than for spread spectrum systems.

For AVCS communication design, it is of crucial importance to make the probability of successful transmission in successive attempts as independent as possible. This helps reducing the probability of a sustained outage of radio link. In particular, the choice of different frequencies per transmission helps substantially. Therefore, slow frequency hopping appears attractive.

The downlink (base station to vehicle) differs from conventional circuit-switched telephone systems. Our criterium is not necessarilly the ouatge probability of loosing a particular packet, because in packet networks, retransmission can repair incidental outages. In our opinion, AVCS systems are to be designed for minimum delay in the exchange of data or to maximaize the rate of updates of vehicle status messages. We conclude that conventional cellular reuse patterns are suboptimum. In packet-oriented communiaction nets, significant performance gains can be achieved if base station carriers are switched off when no packets are available for transmission. This allows the use of access schemes that use the same radio channel in all cells. This concepty is studied for modulation methods that do not use CDMA spreading. In the past, the idea to use the same channel in all cells was believed to be only possible with spread-spectrum transmission. However, we claim that efficient transmission schemes not necessarily use a spreading gain.

The uplink, from vehicle to base station, is not elaborated in full detail. Our main results on the uplink are well derscribed by the findings in a project on the collection of data from probe vehicles for ATMIS purposes. Whenever uplink data traffic is bursty, it appears useful to assign all available bandwidth to all base stations, without any reuse pattern.

This report is organized into 5 chapters. Chapter 1 provides a general introduction to the problem. Chapter 2 formulates a propagation model for vehicle-to-vehicle communication. Chapter 3 reports propagation measurements taken at the Richmond Field Station. Vehicle-to-vehicle communication is addressed in Chapter 4. Chapter 5 covers Base station to vehicle communication.

This final report on MOU 82 is not complete without a reference to related work that is not fully described within the main profile of the MOU, but nonetheless has been carried out in close cooperation.

One such related activity was the design of a single-channel communication architecture. From results reported here, it appeared advantageous to assign the same frequency to neighbouring base stations even if these could harmfully interfere with each other. The bursty character of messaged exchanged in packet-switched AVCS systems appeared to justify a different access methology than what is currently used in cellular telephone systems. The bursty channel occupation allows other users to access the same channel in nearby cells during periods of inactivity. This calls for multiple acces methods that work on the time dimension (within one cell) and in space (to coordinate transmission in different cells). Existing packet access methods mostly do not intregate these two aspects, but split it into two seperate resource assignment methods. Our results here show that this tradition from cellular telephone becomes inefficient for packet switched networks, as foreseen for AVCS. Some concepts that can be used to this end are presented here, but are discussed for more general ITS applications in [6, 7].

The problem of how a large set of base stations, located along a highway, can exploit mutual coordination was a fundamental question raised in MOU 82. One approach to this problem has been suggested by Litjens and Walrand [8].

In the field of vehicle to vehicle communication, we wish to acknowledge the work by Wang and Foreman. Their experiments with off-the-shelf radio modems learned us that the AVCS environment differs essentially from a static environment, as typically encountered for wireless office systems. In particular the requirements for acquisition of synchronisation and keeping the receiver in lock differ substantially. We conclude from these experiments that solutions specific to the fast fading of the AVCS environment are needed. A system that combines DS-CDMA with burst mode transmission was build because many of its compo-

nents were available of the shelf and satisfies FCC requirements for transmission in the bands used. However, this systems needs to resynchronise at every burst transmission and can therefore not achieve high throughput. Reynold designed a slow frequency hopping system that does not have some of these disadvantages. His findings will be reported separately.

While the advantages of direct sequence CDMA cannot easily be fully exploited in a fast fading, lightly dispersive AVCS environment, Multi-Carrier Spread Spectrum Transmission may resolve these problems to some extent. Nathan Yee has contributed to the understanding and performance analysis of MC-CDMA. His finding, tailored to AVCS have been reported in a VTC 1994 paper.

1.2 Acknowledgements

The propagation measurements reported in this document have been made possible by a close cooperation with researchers involved in the INFOPAD project of the Department of E.E.C.S. at the University of California. Also we gratefully acknowledge the support of AT&T for measurement equipment used in the project.

Several graduate students contributed to this work. In particular Rolando Diesta, Tushar Tank, Chikezie Eleazu, Nathan Yee, Reynold Wang and John Davis. Moreover, we appreciate the fruitful discussions and cooperation with other PATH investigators, in particular Jean Walrand at U.C. Berkeley and Andreas Polydoros at U.S.C.

1.3 References

[1] K. Takada, Y. Tanaka, A. Igarashi, and D. Fujita, "Road/Automobile Communication System and its economic effect," *IEEE Vehicle Navigation and Information System Conf.*, pp. A15-21, 1989.

[2] I. Catling and P. Belcher, "Autoguide - route guidance in the United Kingdom.," *IEEE Vehicle Navigation and Information System Conf.*, pp. 467-473, 1989.

[3] W.C. Collier and R.J. Weiland, "Smart cars, smart highways," *IEEE Spectrum*, pp. 27-33,

Apr. 1994.

[4] S. E. Shladover, et al, "Automatic vehicle control developments in the PATH Program," *IEEE Trans. Veh. Technol.*, vol. 40, no. 1, Feb. 1991, pp. 114-130.

[5] A. Polydoros, et al, "Vehicle to roadside communications study", PATH research report PRR-93-4, June 1993.

[6] J.P. Linnartz, "Single Channel Communication Architecture for IVHS", PATH working paper PWP-94-13, 1994.

[7] N. Vvedenskaya and J.P. Linnartz, "Effect of CDMA Transmission on Perfromance of Wireless networks with Stack Algorithm for Collision Resolution", *IEEE Int. Symp. on Personal, Indoor and Mobile Radio Communications*, The Hague, The Netherlands, Sept. 1994, pp. 1129-1132.

[8] R. Litjens, *Conflict-Free Scheduling of Broadcasts in a Linear Packet Radio Network*, Masters Thesis, Dept. of Econometrics, Tilburg University, August 1994.

Chapter 2

Statistical Characterization of Rician Multipath Effects in a Vehicle to Vehicle Communication Channel

This chapter develops a statistical model for a narrowband mobile-to-mobile channel taking into consideration Rician scattering near receiving and transmitting antennas both individually and concomitantly. From the proposed channel model we obtain the probability density function of the received signal envelope, the time correlation function and RF spectrum of the received signal, and level crossing rates and average fade durations. We discuss the impact of these parameters on communication networks supporting an Intelligent Transport System (ITSITS).

2.1 Introduction

The application of microwave data links in a land-to-mobile environment has been shown to suffer from multipath fading, shadowing, and Doppler phase shifts. These effects limit the performance of the system. It is thus desirable to have a model of the channel and its limiting effects. This chapter presents a statistical model for the effects of multipath fading in a mobile-to-mobile environment, extending the statistical model for Rayleigh fading by Clarke [1] and Jakes [4] for mobile-to-land, and by Akki and Haber [7] for mobile-to-mobile communication.

In a mobile channel, energy arrives at the receiver by scattering and diffraction over and/or around the surrounding environment. A short range mobile-to-mobile channel in a highway environment will also contain a much stronger direct line-of-sight component, possibly also with a strong ground reflected wave. These components combine vectorially at the receiver and give rise to a resultant signal that varies greatly depending on the distribution of the phases of the various components. These short-term variations in the received signal are called multipath fading. Long term variations in the signal, such as shadowing or path loss, are also present. The relative motion of the vehicles will give rise to a Doppler shift in the signal. Thus, the mobile radio signal varies rapidly over short distances (fading), with a local mean power that is constant over a small area, but varies slowly as the receiver moves. We will concentrate on the short term effects for narrowband channels. In contrast to [1], [4] and [7], we include a dominant component, resulting in Rician fading.

2.2 Probability Density Function of Received Signal

In deriving the probability density function of the received envelope, we will follow Clarke's two dimensional scattering model [1]. Work has been done by Aulin [11] to extend this to a three dimensional model [9]. However from Aulin's results it is quite clear that those waves which make a major contribution to the received signal travel in an approximately horizontal direction. We will thus continue with Clarke's model which assumes that

the field incident on the mobile antenna is comprised of horizontally travelling plane waves of random phase. Also all reflections occur in a plane and both mobile are at the same height. We will augment Clarke's model by considering a dominant, e.g. line-of-sight, component as well as reflections at both transmitter and receiver. On a highway, reflections may also occur against vehicles in between the transmitter and receiver. However, their signal strength is often much smaller, as the path contains two relatively long segments, each with substantial free space loss. This is similar to the situation in land-to-mobile channels.

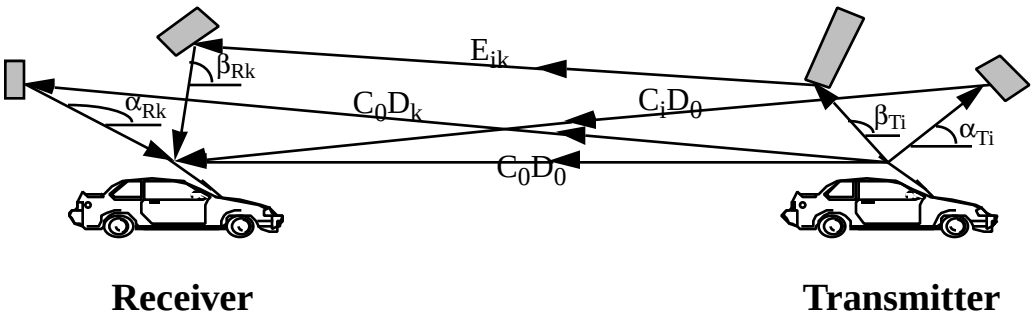

Figure 2.1 Mobile-to-Mobile propagation channel with scatters near both antennas.

At every receiving point we assume the signal to be comprised of many plane waves, as shown in Fig. 2.1. Here N_T waves experience reflections at the transmitter only, N_R waves experience reflections at the receiver only and $N_T N_R$ waves experience reflections at both transmitter and receiver. We denote waves by an index i indicating the path and reflection near the transmitter and an index k denoting the path and reflections near the receiver. The $(i,k)^{th}$ incoming wave has a phase shift $\phi_{i,k}$, a spatial angle of arrival α_{Rk}, and a spatial angle of departure α_{Ti} with respect to the velocity of the receiver. We use $i = 0$ and $k = 0$ for dominant waves that are not subject to scattering. The $(i,k)^{th}$ wave has a real amplitude given by $E_{i,k}$ depending on the reflections and additional path loss that the wave undergoes. In practice the amplitudes $E_{i,k}$ may be difficult to estimate. We model this as $E_{i,k} = E_0 C_{i,k} D_{i,k}$ where $C_{i,k}$ accounts for scattering near the transmitter and $D_{i,k}$ describes scattering near the transmitter. Here $E_0 C_{0,0} D_{0,0}$ is the deterministic amplitude of the dominant component, which in

case it consists only of the line-of-sight wave, is found from free space loss. The parameters $\phi_{i,k}$, α_{Ti}, α_{Rk}, $C_{i,k}$, and $D_{i,k}$ are all assumed to be random and statistically independent, which is reasonable for a sufficiently large separation distance between transmitter and receiver. Maffett [2] has shown that the radar cross section, which is analogous to the dimensionless parameters $C_{i,k}$ and $D_{i,k}$ are a function of polarization and area of incidence. Since the transmitted waves were assumed to be vertically polarized, the area of incidence is the important factor in modelling these parameters. If the separation distance between the two mobiles is sufficiently greater than the distance between mobile and scattering object, the process of scattering at the transmitter and at the receiver may be assumed to be statistically independent. This is particularly the case if the receiver and transmitter are separated sufficiently far to approximate the sum of the waves travelling directly or via one or two reflections as a plane Transversal ElectroMagnetic wave through some plane perpendicular to the transmitter-receiver line of sight. This suggests $C_{i,k} = C_i$ and $D_{i,k} = D_k$. In the following analysis we will consider this to be a special case. Then, $E_{i,k}$ becomes equal to $C_i D_k E_0$, while $E_{i,0}$ and $E_{0,k}$ tend to $C_i D_0 E_0$ and $C_0 D_k E_0$, respectively.

More in general, for reflections at both transmitter and receiver, the signal consists of a double sum over both reflections. If an unmodulated carrier is transmitted, the resulting electric field can be expressed as

$$E(t) = E_{0,0} \cos[(\omega_c + \omega_d)t + \phi_{0,0}] + \sum_{i=1}^{N_T} E_{i,0} \cos[(\omega_c + \omega_{Ti})t + \phi_{i,0}]$$
$$+ \sum_{k=1}^{N_R} E_{0,k} \cos[(\omega_c + \omega_{Rk})t + \phi_k] + \sum_{k=1}^{N_R}\sum_{i=1}^{N_T} E_{i,k} \cos[(\omega_c + \omega_{Rk} - \omega_{Ti})t + \phi_{i,k}] \quad . \quad (1)$$

This field consists of a dominant component, which is treated deterministically, along with components that take into account reflections at the receiver, transmitter, and both receiver and transmitter. Measurements [15] indicated that at short range, both the line-of

sight and the ground reflection are substantially stronger than the sum of weak scattered waves. Reflections off metal surfaces of the vehicle can also be strong. Hence, one may wish to model the channel using deterministic assumptions about strong paths, resulting in $E_{0,0}$, and using a statistical approach for $E_{i,0}$, $E_{0,k}$ and $E_{i,k}$. In Chapter 4, we will use the Rician channel model developed here but we will consider the dominant component $E_{0,0}$ to consist of the phasor sum of the line-of-sight and a ground reflection.

The motion of the transmitter and receiver is evident in a Doppler shift in each wave component. Our model differs from the single reflection (Rayleigh fading) model by Akki and Haber [7]. However, for certain simplifying approximations both models lead to the same result (if the Rician *K*-factor of our model is chosen appropriately). From the geometry of Fig. 2.1, these Doppler shifts are found as follows:

$$\begin{aligned} \omega_d &= \frac{2\pi}{\lambda}\left(V_R\cos\gamma_R - V_T\cos\gamma_T\right) \\ \omega_{Rk} &= \frac{2\pi}{\lambda}V_R\cos\left(\gamma_R - \alpha_{Rk}\right) \quad . \\ \omega_{Ti} &= \frac{2\pi}{\lambda}V_T\cos\left(\gamma_T - \alpha_{Ti}\right) \end{aligned} \tag{2}$$

Here V_T and V_R are the velocities of the transmitter and receiver respectively and γ_T and γ_R are the angles that the motion of transmitter and receiver make with the road axis. In a typical ITS environment vehicles are following each other, thus $\gamma_T = \gamma_R = 0$. The received field can now be expressed as

$$E(t) = I(t)\cos\omega_c t - Q(t)\sin\omega_c t + E_{0,0}\cos\left[\left(\omega_c + \omega_d\right)t + \phi_0\right] \tag{3}$$

where

$$\begin{aligned} I(t) = &\sum_{i=1}^{N_T} E_{i,0}\cos\left(\omega_{Ti}t + \phi_i\right) + \sum_{k=1}^{N_R} E_{0,k}\cos\left(\omega_{Rk}t + \phi_k\right) \\ &+ \sum_{k=1}^{N_R}\sum_{i=1}^{N_T} E_{i,k}\cos\left[\omega_{Rk}t - \omega_{Ti}t + \phi_{i,k}\right] \end{aligned} \tag{4}$$

and

$$Q(t) = \sum_{i=1}^{N_T} E_{0,0} \sin(\omega_{Ti} t + \phi_i) + \sum_{k=1}^{N_R} E_{0,k} \sin(\omega_{Rk} t + \phi_k) + \sum_{k=1}^{N_R} \sum_{i=1}^{N_T} E_{i,k} \sin[\omega_{Rk} t - \omega_{Ti} t + \phi_{ik}] \quad . \tag{5}$$

If N_T and N_R are sufficiently large, in theory infinite (in practice Bennet [3] has shown that greater than 8 paths will suffice), the central limit theorem implies that both *I(t)* and *Q(t)* are Jointly Gaussian random variables for a particular time t and the probability density of the angle of arrivals and departures is uniform between $(-\pi,\pi]$. If we assume that the separation distance between the two mobiles is much larger than the distance between the mobile and scattering object, then Clarke [1] has shown that both *I(t)* and *Q(t)* are uncorrelated and thus independent. The mean values of *I(t)* and *Q(t)* are both zero, the variance of *I(t)* and *Q(t)*, or local-mean scattered power, is given by

$$\sigma^2 = \mathrm{E}\left[\sum_{i=1}^{N_T} \frac{E_{i,0}^2}{2} + \sum_{k=1}^{N_R} \frac{E_{0,k}^2}{2} + \sum_{i=1}^{N_T} \sum_{k=1}^{N_R} \frac{E_{i,k}^2}{2}\right] \tag{6}$$

and they are jointly Rayleigh distributed. Following Rice [6] we find that the joint probability density function of the received amplitude, $r(t)$, and phase, $\theta(t)$, is

$$f_{r,\theta}(r,\theta) = \frac{r}{2\pi\sigma^2} \exp\left(\frac{-(r^2 - 2rE_{0,0}\cos(\theta - \omega_d t) + E_{0,0}^2)}{2\sigma^2}\right) \tag{7}$$

and thus the probability density function of the amplitude is given by

$$f_r(r) = \frac{r}{\sigma^2} \exp\left(\frac{-(r^2 + E_{0,0}^2)}{2\sigma^2}\right) I_0\left(\frac{rE_{0,0}}{\sigma^2}\right) \tag{8}$$

where $I_0(.)$ is defined as the modified zero-order Bessel function of the first kind. We further

define the Rician K factor as the ratio of the power in the direct line-of-sight component to the local-mean scattered power

$$K = \frac{E_{0,0}^2}{2\sigma^2} \tag{9}$$

and define the local-mean power as

$$\bar{p} = \frac{1}{2}E_{0,0}^2 + \sigma^2 = P_D + P_R + P_T + P_B \tag{10}$$

where P_D, P_T, P_R and P_B are the portions of the local mean power in the dominant path, the waves that are scattered only near the transmitter, those scattered only near the receiver and those scattered twice, respectively. The pdf of the signal envelope r can be expressed as

$$f_r(r) = r\frac{(1+K)}{\bar{p}}\exp\left(\frac{-K(1+K^2)r^2}{2\bar{p}}\right)I_0\left(r\sqrt{\frac{2K(1+K)}{\bar{p}}}\right) . \tag{11}$$

For the special case of sufficiently large antenna separation, we may further define Rician K factors at the receiver and transmitter as the ratio of the power in the direct line-of-sight wave and the local-mean scattered power at the receiver and transmitter respectively, with

$$K_R = \frac{D_0^2}{\mathrm{E}\left[\sum_{i=0}^{N_R} D_i^2\right]} \tag{12}$$

and

$$K_T = \frac{C_0^2}{\mathrm{E}\left[\sum_{i=0}^{N_T} C_i^2\right]}. \tag{13}$$

The pdf of the signal envelope can be expressed in terms of these new Rician K factors by making the following substitution of variables

$$K = \frac{K_R K_T}{K_T + K_R + 1 + K_R K_T} \quad . \tag{14}$$

We note that the resulting fading is Rician, which is similar to the case of a line-of-sight component with reflections occurring only at one of the antennas. Reflections at both transmitter and receiver are subject to two Doppler shifts. This results in a larger variance in both the in-phase and quadrature field components, which is tantamount to an increase in the scattered mean power.

2.3 RF Spectrum

The transmitted signal will be subject to Doppler shifts in the various paths. These Doppler shifts will tend to spread the bandwidth of the transmitted signal, which will be evident in the RF spectrum. The RF spectrum can be found by taking the Fourier transform of the temporal autocorrelation function of the electric field, the latter defined as

$$\mathrm{E}\left[E(t)\,E(t+\tau)\right] . \tag{15}$$

Following Clarke [1], if we let

$$a(\tau) = \mathrm{E}\left[I(t)\,I(t+\tau)\right] = \mathrm{E}\left[Q(t)\,Q(t+\tau)\right] \tag{16}$$

and

$$c(\tau) = \mathrm{E}\left[I(t)\,Q(t+\tau)\right] = -\mathrm{E}\left[Q(t)\,I(t+\tau)\right] \tag{17}$$

then the autocorrelation can be expressed as

$$\mathrm{E}\left[E(t)\,E(t+\tau)\right] = a(\tau)\cos\omega_c\tau - c(\tau)\sin\omega_c\tau + E_{0,0}^2\cos\left(\omega_c + \omega_d\right)\tau \tag{18}$$

The parameters C_n, D_n, and ϕ_n are statistically independent, due to the large separation distance between mobiles and the fact that small changes in path length will yield large changes in phase. Thus the following simplification can be made

$$a(\tau) = P_R\mathrm{E}\left[\cos\omega_R\tau\right] + P_T\mathrm{E}\left[\cos\omega_T\tau\right] + P_B\mathrm{E}\left[\cos\left(\omega_T\tau - \omega_R\tau\right)\right] \tag{19}$$

$$c(\tau) = P_R\mathrm{E}\left[\sin\omega_R\tau\right] + P_T\mathrm{E}\left[\sin\omega_T\tau\right] + P_B\mathrm{E}\left[\sin\left(\omega_T\tau - \omega_R\tau\right)\right] \tag{20}$$

A critical assumption in [1] is that, for a large number of waves arriving at the receiver and departing at the transmitter, waves are modelled to arrive (or depart) from all angles in the azimuth plane with uniform probability density. For short range vehicle-to-vehicle communication this assumption is less obvious than for macro-cellular propagation environments.

If, for ease of analysis, the probability density functions for α_T and α_R are nonetheless modelled by an independent uniform distribution between $(-\pi,\pi]$, we can now evaluate the above expectations as

$$a(\tau) = P_R J_0[2\pi f_{MR}\tau] + P_T J_0[2\pi f_{MT}\tau] + P_B J_0[2\pi f_{MT}\tau] J_0[2\pi f_{MR}\tau] \quad (21)$$

$$c(\tau) = 0 \quad (22)$$

where $J_0(.)$ is the zero-order Bessel function of the first kind and f_{MR} and f_{MT} are the maximum Doppler shifts at the transmitter and receiver respectively given by

$$f_{MT} = V_T/\lambda \quad (23)$$

and

$$f_{MR} = V_R/\lambda. \quad (24)$$

The fact that $c(\tau)$ is zero is a mathematical consequence of sin(.) being an odd function. Physically this result can be related to the fact that the RF spectrum is symmetric about f_c. In order to calculate the power spectral density of *I(t)* and *Q(t)* we must first find the Fourier transform of $a(\tau)$. The Fourier transform of the first two terms can be found from Gradshteyn and Ryzhik [5,p.707] as

$$F\{P_R J_0[2\pi f_{MR}\tau] + P_T J_0[2\pi f_{MT}\tau]\} = \frac{P_R}{2\pi\sqrt{f_{MR}^2 - f^2}}\Pi\left(\frac{f-f_c}{2f_{MR}}\right) + \frac{P_T}{2\pi\sqrt{f_{MT}^2 - f^2}}\Pi\left(\frac{f-f_c}{2f_{MT}}\right) \quad (25)$$

where $\Pi(f/x)$ is the rectangular pulse function centered at $f = 0$ with a width of x and unity

amplitude. The transform of the third term can be found [5, p.709] as

$$F\{P_B J_0[2\pi f_{MR}\tau]\, J_0[2\pi f_{MT}\tau]\} = \frac{P_B}{2\pi^2\sqrt{f_{MT}f_{MR}}} Q_{-1/2}\left(\frac{f_{MR}^2 + f_{MT}^2 - f^2}{2f_{MR}f_{MT}}\right)\Pi\left(\frac{f - f_c}{2f_{MR} + 2f_{MT}}\right) \quad (26)$$

where $Q_{-1/2}(.)$ is the Legendre function of the second kind. By using the following identity found [5]

$$Q_{-1/2}(x) = K\left(\sqrt{\frac{1+x}{2}}\right), \quad (27)$$

the above transformation can be written in terms of K(.), the complete elliptical integral of the first kind, as

$$F\{P_B J_0[2\pi f_{MR}\tau]\, J_0[2\pi f_{MT}\tau]\} = \frac{P_B}{2\pi^2\sqrt{f_{MT}f_{MR}}} K\left(\sqrt{\frac{(f_{MR}+f_{MT})^2 - f^2}{4f_{MR}f_{MT}}}\right)\Pi\left(\frac{f - f_c}{2f_{MR} + 2f_{MT}}\right). \quad (28)$$

Setting $V_T = 0$ we get an expression analogous to the expression in [1, p.969] for the baseband output spectrum from a square law detector. This output spectrum appears to be the convolution of the input spectrum with itself. This argument can be applied to our result. Namely the spectral contribution to the RF spectrum of the waves that undergo reflections at both receiver and transmitter, can be viewed as the convolution of the spectral components that undergo reflections only at the receiver with the spectral components that undergo reflection only at the transmitter. Stated mathematically,

$$F\{P_B J_0[2\pi f_{MR}\tau]\, J_0[2\pi f_{MT}\tau]\} = P_B\{F(J_0[2\pi f_{MR}\tau]) \otimes F(J_0[2\pi f_{MT}\tau])\}. \quad (29)$$

The RF spectrum can now be found by noting that $a(\tau)$ is modulated by $\cos\omega_c\tau$, thus

shifting the spectrum of $a(\tau)$ by the carrier frequency, and the direct line-of-sight wave will give rise to a delta function since this wave will only undergo a deterministic Doppler shift. Thus the RF spectra can be written as

$$S_{RF}(f) = F\{a(\tau)\cos\omega_c\tau + 2P_B[\cos(\omega_c + \omega_d)\tau]\} \tag{30}$$

or

$$\begin{aligned} S_{RF}(f) &= \frac{P_R}{2\pi\sqrt{f_{MR}^2 - (f-f_c)^2}}\Pi\left(\frac{f-f_c}{2f_{MR}}\right) + \frac{P_T}{2\pi\sqrt{f_{MT}^2 - (f-f_c)^2}}\Pi\left(\frac{f-f_c}{2f_{MT}}\right) \\ &+ \frac{P_B}{2\pi^2\sqrt{f_{MT}f_{MR}}}\mathrm{K}\left(\sqrt{\frac{(f_{MR}+f_{MT})^2-(f-f_c)^2}{4f_{MR}f_{MT}}}\right)\Pi\left(\frac{f-f_c}{2f_{MR}+2f_{MT}}\right) + P_D 2\pi\delta(f-f_c-f_{MD}) \end{aligned} \tag{31}$$

where the Doppler shift of the direct line-of-sight component is

$$f_{MD} = f_{MR}\cos\gamma_R + f_{MT}\cos\gamma_T\,. \tag{32}$$

In Fig. 2.2, we see that the RF spectrum is centered around the carrier frequency and bandlimited to $2(f_{MT} + f_{MR})$ which is a direct consequence of the Doppler shift incurred by the movement of transmitter and receiver.

The probability densities of α_R and α_T affect the shape of the spectrum inside this band. If we set $V_T = 0$ we do not obtain Clarke's spectrum for a mobile receiver and stationary transmitter. This is due to the fact that Clarke's model assumes no scattering at the transmitter. However if we set the Rician factors K_T and K_R to zero, we obtain a spectrum analogous to that of Akki and Haber [7] for a Rayleigh fading channel with scattering at transmitter and receiver only.

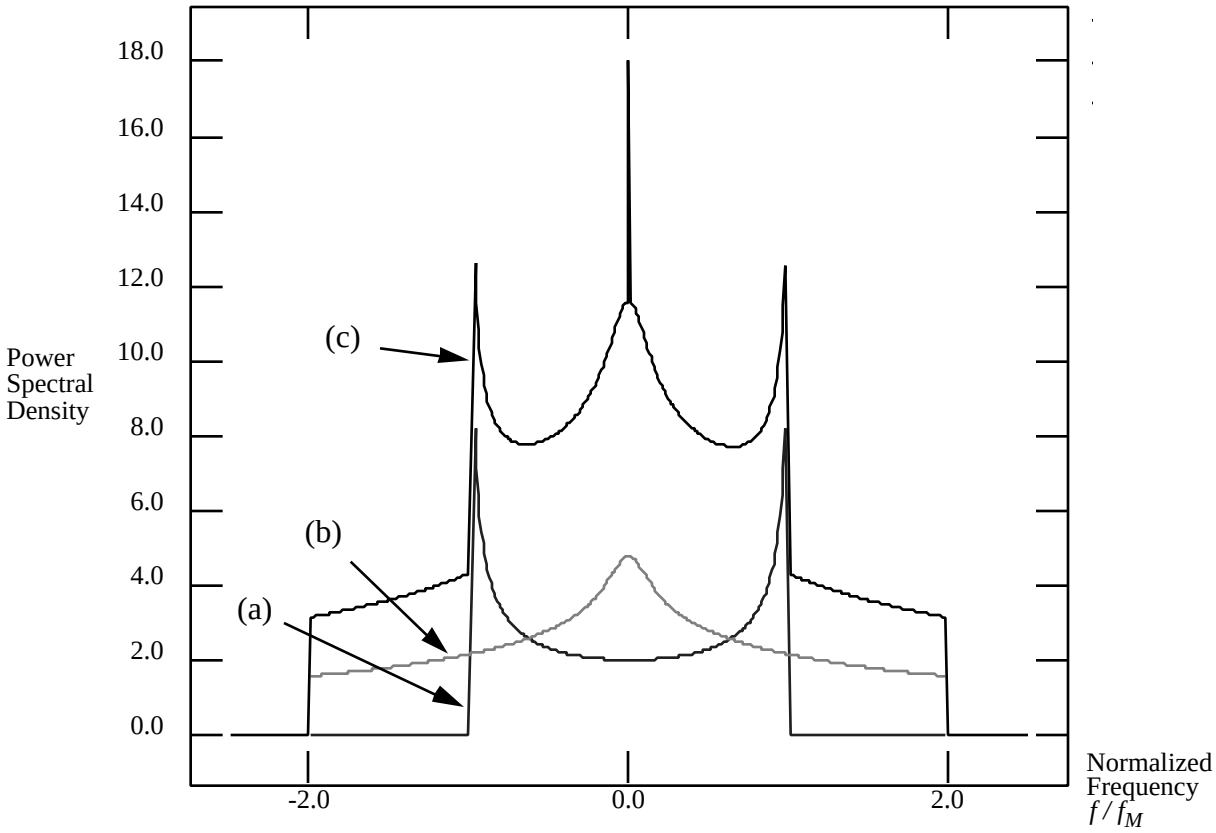

Figure 2.2 RF Spectra of mobile-to-mobile radio channel with equal transmitter and receiver velocities. (a) Reflections solely at either receiver or transmitter. (b) Reflections at both receiver and transmitter (c) summation of (a) and (b).

2.4 Moments of Power Spectral Density

The correlation functions $a(\tau)$ and $c(\tau)$ defined earlier can be expressed as inverse Fourier transforms of the power spectral density without the line-of-sight component as

$$a(\tau) = \int_{f_c-(f_{MT}+f_{MR})}^{f_c+(f_{MT}+f_{MR})} S_i(f) \cos[2\pi(f-f_c)\tau]\, df \tag{33}$$

$$c(\tau) = \int_{f_c-(f_{MT}+f_{MR})}^{f_c+(f_{MT}+f_{MR})} S_i(f) \sin[2\pi(f-f_c)\tau]\, df \tag{34}$$

where

$$S_i(f) = S_{RF}(f) - E_{0,0}^2 \pi\delta(f - f_c - f_{MD}) \tag{35}$$

It was shown before that *c(t)* is zero for all *t*. This can further be explained from the above equation since the RF spectrum is an even function while sin(.) is odd. Evaluation of these autocorrelations at zero will give the moments of the power spectrum. Following Jakes [4]

$$\mathrm{E}[I^2(t)] = \mathrm{E}[Q^2(t)] = a(0) = b_0 = P_B + P_T + P_R$$

$$\mathrm{E}[I(t)Q(t)] = c(0) = 0$$

$$\mathrm{E}[I(t)\dot{I}(t)] = \mathrm{E}[Q(t)\dot{Q}(t)] = \dot{a}(0) = 0$$

$$\mathrm{E}[I(t)\dot{Q}(t)] = -\mathrm{E}[\dot{I}(t)Q(t)] = \dot{c}(0) = b_1 = 0$$

$$\mathrm{E}[\dot{I}^2(t)] = \mathrm{E}[\dot{Q}^2(t)] = -\ddot{a}(0) = b_2$$

$$= \frac{1}{2}(P_T\omega_{MT}^2 + P_R\omega_{MR}^2 + P_B(\omega_{MT} + \omega_{MR})^2) \tag{36}$$

where the (over) dots represent differentiation with respect to time. Thus $b_n = 0$ for all odd n, again due to the symmetric nature of $S_{RF}(f)$. The moments of the power spectrum for even n can be generalized as

$$b_n = \left(\frac{1 \cdot 3 \cdot 5 \ldots n-1}{2 \cdot 4 \cdot 6 \ldots n}\right)(P_T\omega_{MT}^n + P_R\omega_{MR}^n + P_B(\omega_{MT} + \omega_{MR})^n) \quad . \tag{37}$$

Using the results of (37) we can now investigate the derivatives of the in-phase and quadrature components: specifically, to derive the joint pdf of these components and their derivatives. The in-phase and quadrature components and their derivatives are zero-mean Jointly Gaussian. The covariance matrix can be expressed as

$$\boldsymbol{V} = \begin{bmatrix} a(0) & c(0) & \dot{a}(0) & \dot{c}(0) \\ c(0) & a(0) & -\dot{c}(0) & \dot{a}(0) \\ \dot{a}(0) & -\dot{c}(0) & -\ddot{a}(0) & \ddot{c}(0) \\ \dot{c}(0) & \dot{a}(0) & \ddot{c}(0) & -\ddot{a}(0) \end{bmatrix} = \begin{bmatrix} b_0 & 0 & 0 & 0 \\ 0 & b_0 & 0 & 0 \\ 0 & 0 & b_2 & 0 \\ 0 & 0 & 0 & b_2 \end{bmatrix} \tag{38}$$

so

$$\boldsymbol{V}^{-1} = \left(\frac{1}{b_0^2 b_2^2}\right) \begin{bmatrix} b_0 b_2^2 & 0 & 0 & 0 \\ 0 & b_0 b_2^2 & 0 & 0 \\ 0 & 0 & b_0^2 b_2 & 0 \\ 0 & 0 & 0 & b_0^2 b_2 \end{bmatrix} . \tag{39}$$

The joint pdf [6],[10] can be written as

$$f_{I,Q,\dot{I},\dot{Q}}(I, Q, \dot{I}, \dot{Q}) = \frac{1}{4\pi^2 b_0 b_2} \exp\left(\frac{-1}{2b_0 b_2}[b_2(I^2 + Q^2) + b_0(\dot{I}^2 + \dot{Q}^2)]\right). \tag{40}$$

The in-phase and quadrature components can be expressed in terms of an amplitude r and phase θ as follows

$$\begin{aligned} I(t) &= r\cos\theta - E_{0,0}\cos(\omega_d t + \phi) \\ Q(t) &= r\sin\theta - E_{0,0}\sin(\omega_d t + \phi) \\ \dot{I}(t) &= \dot{r}\cos\theta - r\dot{\theta}\sin\theta \\ \dot{Q}(t) &= \dot{r}\sin\theta - r\dot{\theta}\cos\theta \end{aligned} . \tag{41}$$

The joint pdf of the amplitude, phase and derivatives can be expressed as

$$f_{r,\theta,\dot{r},\dot{\theta}}(r, \theta, \dot{r}, \dot{\theta}) = \frac{r^2}{4\pi^2 b_0 b_2} \exp\left\{\frac{-1}{2b_0 b_2}[b_2 r^2 - 2rE_{0,0}\cos(\omega_d t + \theta) + E_{0,0}^2] + b_0(\dot{r}^2 + r^2\dot{\theta}^2)\right\} . \tag{42}$$

If we uncondition this expression over the phase and both derivatives, we obtain the same expression for the pdf of the signal envelope derived earlier (with $b_0 = \sigma^2$).

2.5 Level Crossing Rate and Average Fade Duration

The fading of the signal envelope was evident in the derivation of the probability density function of the envelope. From this pdf we can obtain an expression for the overall percentage of time that the envelope lies below a certain level and on average how long these fades last. We are also interested in finding the rate at which the envelope crosses a particular level R. These expressions would thus provide parameters in selecting transmission bit rates, word lengths and coding schemes. The level crossing rate, L_R, is defined as the expected number of times per second that the envelope crosses R in the positive direction. Rice [6] gives this value as

$$L_R = \int_0^\infty \dot{r} f_{r,\dot{r}}(R, \dot{r})\, d\dot{r} \ . \tag{43}$$

Thus we must first find the joint pdf of the envelope and its derivative. This can be derived by integrating the phase and its derivative over the joint pdf derived earlier.

$$\begin{aligned} f_{r,\dot{r}}(r, \dot{r}) &= \int_{-\infty}^{\infty}\int_0^{2\pi} f_{r,\theta,\dot{r},\dot{\theta}}(r, \theta, \dot{r}, \dot{\theta})\, d\theta d\dot{\theta} \\ &= \frac{r}{b_0} I_0\left(\frac{rE_{0,0}}{b_0}\right) \exp\left[\frac{-(r^2 + (E_{0,0})^2)}{2b_0}\right] \times \frac{1}{\sqrt{2\pi b_2}} \exp\left(\frac{-\dot{r}^2}{2b_2}\right) \end{aligned} \tag{44}$$

From this expression we see that since both the envelope and its derivative are independent and thus uncorrelated, their joint pdf can be expressed as the product of individual pdf's. Thus the derivative of the envelope is zero-mean Gaussian with a variance of b_2 and the pdf of the envelope is the same as before. The level crossing rate then be expressed as

$$L_R = \frac{R}{b_0}\sqrt{\frac{b_2}{2\pi}} I_0\left(\frac{R \cdot E_{0,0}}{b_0}\right) \exp\left[\frac{-(R^2 + E_{0,0}^2)}{2b_0}\right] \quad . \tag{45}$$

We further define the fade margin as the ratio of the mean signal power to the specified level, R. Fig. 2.3 plots the normalized level crossing rate, L_R/f_M or level crossings per wavelength, for various Rician K factors.

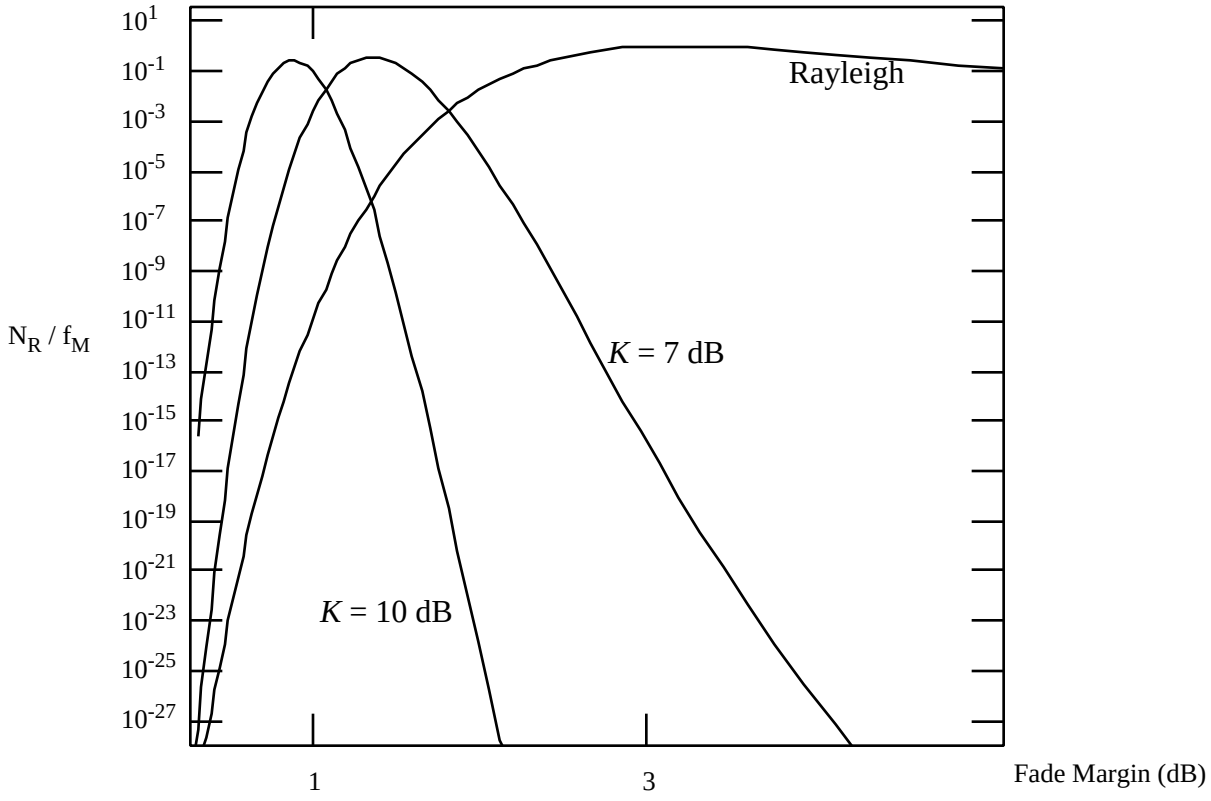

Figure 2.3 Normalized Level Crossing Rate vs. Fade Margin for various Rician K factors. Equal transmitter and receiver velocities. Equal Rician K factors K_R and K_T.

Another important statistical measure of the envelope is the average fade duration. The fade duration, τ, below a specified level R, is defined as the period of fade below this level. The overall fraction of time for which the signal is below a specified level R is given by the cumulative distribution function, $F_r(R)$, of the received signal envelope. This function is obtained by integrating over the pdf of the envelope

$$F_r(R) = \int_0^R f_r(r)\,dr \quad . \tag{46}$$

The average fade duration can now be expressed as [9]

$$E[\tau_r] = \frac{F_r(R)}{L_R} \quad . \tag{47}$$

Fig. 2.4 plots the normalized average fade durations for various Rician K factors.

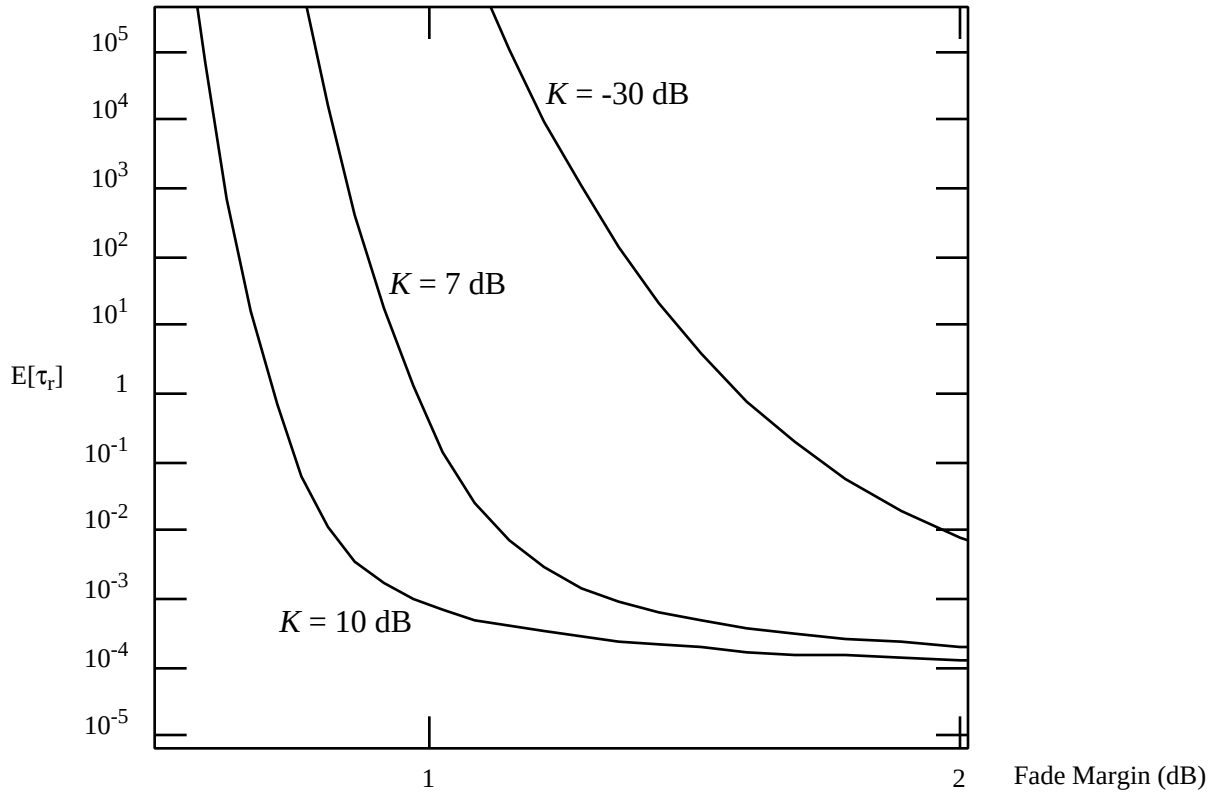

Figure 2.4 Average Fade Duration vs. Fade Margin for various K factors. Equal transmitter and receiver velocities. Equal Rician K factors K_R and K_T. Maximum Doppler shift for both antennas, f_M.

2.6 Conclusions

A statistical model for a mobile-to-mobile channel has been presented that extends the work on Rayleigh fading channels, without a line-of-sight component, by Clarke [1], Jakes

[4], and Akki and Haber [7]. The channel model examines multipath fading and Doppler shifts for a narrowband signal taking into consideration scatters at both receiving and transmitting antennas both individually and concomitantly, as well as a strong line-of-sight component between antennas. This is in contrast to the model by Akki and Haber [7] which focussed on single reflections, ignoring a LOS or double reflections. The proposed model loses some of its accuracy when the transmit and receive antennas become too close. This suggests that the special case addressed here for independent scattering at the transmitter and receiver may be better acceptable for platoon-to-platoon communications, but needs further verification or it may need refinement for communication within a platoon.

Even with scattering at both transmitter and receiver, the line-of-sight component causes the fading to be Rician, with a new Rician K factor that is a function of the K factors at the transmitter, K_T, and receiver, K_R. As K_T and K_R approach zero we obtain results analogous to Akki and Haber [7] for Rayleigh fading with long range reflections. Also Doppler spreads, for vehicles travelling at roughly the same speed, are twice as large as those reported in text books like [4], thus the fading has components that are twice as fast. We interpret from our curves that fade durations longer than 50 msec diminish rapidly with fade margin. This implies that, if the fade margin is sufficiently large, the probability that the radio link is in an outage for longer than 50 msec is very small. In an AVCS system, it appears important that longer outages become unlikely [14].

2.7 References

[1] R.H. Clarke, "A Statistical Theory of Mobile Radio Reception", *Bell. Syst. Tech. J.*, pp. 957-1000, July 1968.

[2] A.L. Maffett, *Topics for a Statistical Description of Radar Cross Section*, New York: Wiley, 1989.

[3] W. R. Bennet, "Distribution of the Sum of Randomly Phased Components", *Quart. Appl. Math.*, vol. 5, 1948, pp. 385-395.

[4] W.C. Jakes (Ed.), *Microwave Mobile Communication*, New York: Wiley, 1974.

[5] I.S. Gradshteyn and I.M. Ryzhik, *Tables of Integrals, Series and Products*, New York: Academic Press, 1965.

[6] S.O. Rice, "Statistical properties of sine wave plus random noise," *Bell Syst. Tech. J.*, Jan. 1948, pp. 292-332.

[7] A.S. Akki and F. Haber, "A statistical model of mobile to mobile land communication channel," *IEEE Trans. Veh. Technol.*,vol. 35, no. 1, 1986, pp. 2-7.

[8] F. Bowman, *Introduction to Bessel Functions*, New York: Dover, 1958.

[9] D. Parsons, *The Mobile Radio Propagation Channel*, New York: Wiley, 1992.

[10] A. Leon-Garcia, *Probability and Random Processes for Electrical Engineering*, New York: Addison-Wesley, 1989.

[11] T. Aulin, "A modified model for the fading signal at a mobile radio channel," *IEEE Trans. Veh. Technol.*, vol. 28, no. 3, 1979, pp. 182-203.

[12] W.B. Davenport and W.L. Root, *An Introduction to the Theory of Random Signals and Noise*, New York: McGraw-Hill, 1958.

[13] J.P.M.G. Linnartz, *Narrowband Land-Mobile Radio Networks*, Boston: Artech House, 1993.

[14] S. E. Shladover, et al, "Automatic vehicle control developments in the PATH Program," *IEEE Trans. Veh. Technol.*, vol. 40, no. 1, Feb. 1991, pp. 114-130.

[15] J.S. Davis II and J.P.M.G. Linnartz, "Vehicle-to-vehicle RF propagation measurements", *28th Asilomar Conf. on Signals, Systems, and Computers*, Pacific Grove, California, Nov. 1994, pp. 470-474.

Chapter 3

Vehicle to Vehicle RF Propagation Measurements

This chapter presents results from vehicle to vehicle RF propagation measurements in the 900 MHz band focusing on determining delay spread, probability distribution parameters (in particular, the Rician *K* factor) and path loss rates. The parameters and results are discussed with implications for the use of RF communication between automobiles in AVCS.

3.1 Introduction

The purpose of this chapter is to present propagation measurements of RF signals between vehicles. The results help determine the feasibility of using RF communication between vehicles in platoons. The organization of this chapter is as follows. Section 3.2 is a review of RF propagation theories. Section 3.3 outlines the measurement procedure and presents the measurement results. Section 3.4 discusses the results and presents some conclusions.

3.2 RF Propagation Review

A great deal of literature is available on RF mobile propagation [1 - 16]. Much of the work has been focused on transmission between users in automobiles to and from a shared base station [1, 7, 8]. In such scenarios, transmission distances can be quite large, often measured in terms of city blocks. Furthermore, a line of sight (LOS) path between the transmitter and the receiver is not always likely as the base station antenna is often blocked by buildings and other obstacles. The channel is quite different when considering vehicle to vehicle communication. Based on the proposed platoon structures, it can be assumed that the transmission distances will be quite small compared to the RF transmission cases cited above. In addition, a LOS signal path is virtually guaranteed since any obstacles in the roadway would not only be harmful to RF transmission, but also to driver safety.

There are several causes of signal corruption in a wireless channel. Fundamentally, three of the primary causes of corruption are signal attenuation due to distance, multipath reception and channel time variation. Signal attenuation over distance is observed when the mean received signal power is attenuated as a function of the distance from the transmitter. The most common form of this is often called free space loss and is due to the signal power being spread out over the surface area of an expanding sphere as the receiver moves farther from the transmitter.

Multipath transmission results from the fact that the transmission channel consists of

several obstacles and reflectors. Thus, the received signal arrives as a set of reflections and/or direct waves each with its own degree of attenuation and delay. Delay spread, T_D, is a parameter commonly used to quantify multipath effects. Informally, delay spread is the difference in time between the first and last received signals from the transmitter to the receiver. More formally we consider the RMS and Mean Excess delay spread in which the instantaneous impulse response is treated like a probability distribution function (pdf). Multipath transmission manifests itself as variation in the received signal strength over frequency. Often researchers consider the coherence bandwidth as a measure of how much the received power level varies in the frequency domain. Coherence bandwidth appears to be inversely proportional to the delay spread.

Time variation of the channel is due to the assumption that the communicating vehicles are in motion. Closely related to Doppler shifting, time variation in conjunction with multipath transmission leads to variation of the instantaneous received signal strength about the mean power level as the receiver moves over distances on the order of less than a single carrier wavelength. Given that the vehicles are in motion, time variation of the channel is realized as spatial variation and becomes uncorrelated approximately every half carrier wavelength over distance.

The variation of received signal amplitude in the time domain observes a probability distribution in one of two forms. The first form, Rayleigh fading, generally occurs when there is no direct line-of-sight path between the transmitter and the receiver. The second and more general form of multipath fading is Rician fading and occurs when a line-of-sight path is present. A Rician distribution consists of two parameters; the Rician *K* factor and local mean signal power. The *K* factor is defined as the ratio of the direct line-of-sight signal strength to the scattered (reflected) signal components. For Rayleigh fading, the *K* factor is zero and thus the Rician distribution reduces mathematically to a Rayleigh distribution.

3.2.1 Base Station to Vehicle Channel Model

The correct reception of transmitted data depends on the signal power relative to the background noise in the channel, and any interfering signals. It is hence important to characterize the spatial power variation in the channel. Four propagation mechanisms influence mobile radio reception:

1. Large Scale Attenuation.

2 The Shadowing Effect.

3. Channelling Effects.

4. Multipath Fading.

3.2.1.1 Large Scale Attenuation

We model the propagation channel as a dominant direct component, with an amplitude determined by path loss, a set of early reflected waves adding coherently with the dominant wave, and intersymbol interference caused by the excessively delayed waves, adding incoherently with the dominant wave. We learn from propagation models proposed for micro-cellular communication that the path loss shows a transition from free-space loss to a ground wave propagation. Free-space loss is experienced if $r\lambda < 4h_r h_t$ where r represents the distance from the transmitter, λ is the wavelength of the carrier wave, and h_r & h_t are respectively the heights of the receiving and transmitting antennas. Harley [20] suggested a smooth transition, with

$$\bar{p} = r^{-\beta_1}\left(1 + \frac{r}{r_g}\right)^{-\beta_2} \tag{1}$$

where r_g is the normalized turn over distance, and $\bar{p}$ is the local-mean power (i.e., received power averaged over a few meters). Studies done by [15] indicate that actual turn over distances on the order of 800 meters are reasonable around 2 GHz. Other models, such as a stepwise transition, have been proposed. Empirical values for β_1 and β_2 have been reported e.g. [21]. The smooth transition in (1) is assumed in this chapter with $\beta_1 = 2$ and $\beta_2 = 2$.

3.2.1.2 Shadowing Effect

The shadowing effect refers to the fluctuation of the local-mean power about the area-mean power (i.e., received power averaged over tens to hundreds of meters) due to large scale reflections. Due to the limited (micro-cellular) transmission distances involved with the Intelligent Vehicle/Highway Systems, there will generally be a line-of-sight (LOS) path between the transmitter and receiver. A factor to consider is obstruction due to traffic on the highway. Studies in [15] show that the shadowing effects in the AVCS environment do not necessarily give rise to the log-normal distribution of the local-mean power as is the case in the usual macro-cellular environments. Further, shadowing and multipath appear not to behave as independent processes [15]. Calculations in [15] to determine the received power involve determining which rays are obstructed (if any) and subsequently using a specific Multi-Ray model. In the extreme case of an obstruction of the LOS and ground waves, the power is Rayleigh distributed. In this chapter, we will make the assumption that there is always a line-of-sight path.

3.2.1.3 Channelling Effects

Specular reflections from near and far walls that are typical along highways lead to fairly quick variations of power with distance [15]. In this report, this effect is lumped with multipath fading (explained next).

3.2.1.4 Multipath Fading

The base stations in PATH ITS are assumed to be transmitting to vehicles within distances on the order of a few hundred meters. The channel is also characterized by the presence of multipath reflections due to the relatively low antenna positions. The received signals hence consist of a dominant line-of-sight component and reflections of the transmitted signals. This leads to rapid power fluctuations as the vehicle moves within the coverage area of the base station. In this chapter, only narrowband channels are considered. This

implies that the interarrival times of the reflected waves are small compared to the variations in the modulating signal. The reflected waves hence add coherently. RMS delay spreads on the order of 1 ns have been computed [15] for the AVCS environment at carrier frequencies around 1800 MHz. The coherence bandwidth is hence around 100 MHz. Given the assumption of bit rates of up to 80 kHz between vehicles and base stations, the narrowband assumption is reasonable. RMS delay spreads longer than 1 ns have been reported; e.g., 300 ns is reported for small city microcells [22]. The narrowband assumption is still valid for this value.

Rician fading occurs in a channel if the central limit theorem can be applied to the reflected waves. This in turn only occurs if the number of reflected waves is large, and none of them dominates the joint reflected power. Considering the characteristics of the channel described above, Rician fading is a good assumption.

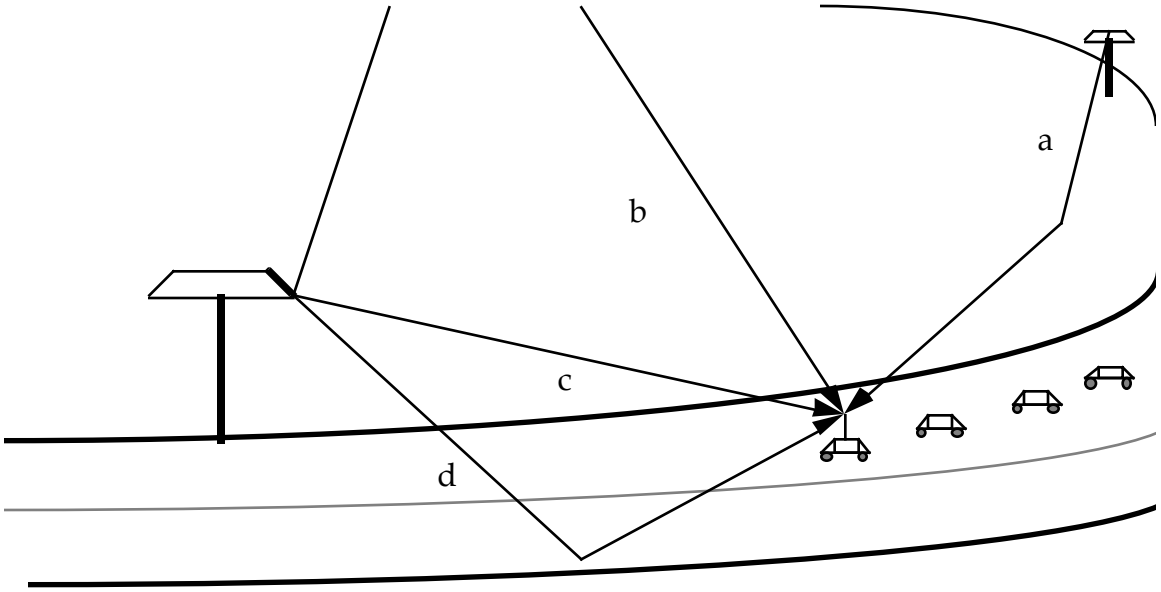

Figure 3.1 Channel Model. Ray Paths: (a) Rayleigh fading co-channel interference, (b) excessively delayed path, (c) line-of-sight (L.O.S.) path, (d) first resolvable path.

3.2.2 Vehicle to Vehicle Channel Model

3.2.2.1 Attenuation Models

Vehicle-to-vehicle data communication will mainly consist of the continuous (routine) exchange of telemetric data such as vehicle status, speed, and acceleration. Interfering signals will be present from vehicles within the platoon and from outside the platoon (from vehicles in other lanes). Vehicles with bumper mounted directional antennas are considered.

The vehicle-to-vehicle radio link can be modelled statistically as a Rician fading channel. The dominant component in the Rician fading channel is likely to be relatively strong compared to the reflected signal (large Rician K-factor), and the delay spread is likely to be relatively small because reflections occur in the immediate vicinity of the transmitter and receiver antenna. The propagation channel is modelled as a dominant component consisting of a direct-line-of-sight wave and a ground reflected wave, a set of early reflected waves, and intersymbol interference caused by excessively delayed waves.

Propagation models proposed for micro-cellular communication, model path loss with a transition from free-space propagation to groundwave propagation if $d\lambda < 4h_r h_t$, where d is the distance of the radio link under study, h_r and h_t are the heights of the receiving and transmitting antenna respectively, and λ is the wavelength of the transmitted wave. Various models have been proposed, e.g. a step-wise transition from $\beta_1 = 2$ to $\beta_2 = 4$ (empirical values) at a certain (turnover) distance d_g. Harley's [20] smooth transition, has been described earlier. However when the distance between the receiver and antenna is small and unobstructed the direct line-of-sight component and the ground reflected component will cause strong fluctuations in the received signal power due to mutual interference between these two waves. Thus the local mean power of the dominant wave does not show a smooth transition between free-space and groundwave propagation. Rather this transition is marked by strong fluctuations in the local mean power.

3.2.2.2 Path Loss Near a Dielectric Surface

The road surface is neither a perfect conductor nor dielectric so the reflection coefficient depends on the dielectric constant ε and the conductivity σ of the road surface. In order to facilitate computation we assume the road surface to be smooth and thus the dielectric constant and conductivity do not vary with distance. The reflection coefficient for horizontally polarized waves is given by [23]

$$\Gamma = \frac{\sin\Theta - \sqrt{\left(\frac{\varepsilon}{\varepsilon_0} - j\frac{\sigma}{\omega\varepsilon_0}\right) - (\cos\Theta)^2}}{\sin\Theta + \sqrt{\left(\frac{\varepsilon}{\varepsilon_0} - j\frac{\sigma}{\omega\varepsilon_0}\right) - (\cos\Theta)^2}} \quad , \tag{2}$$

where ω is the angular frequency of the signal, ε_0 is the dielectric constant of free space and Θ is the angle of incidence, which we assume to be equal to the angle of reflection, and

$$\chi = \frac{\sigma}{\omega\varepsilon_0} = \frac{18\times10^9\sigma}{f}. \tag{3}$$

For vertical polarization the reflection coefficient is given by [23]

$$\Gamma = \frac{(\varepsilon_r - j\chi)\sin\Theta - \sqrt{(\varepsilon_r - j\chi) - (\cos\Theta)^2}}{(\varepsilon_r - j\chi)\sin\Theta + \sqrt{(\varepsilon_r - j\chi) - (\cos\Theta)^2}}. \tag{4}$$

Since this reflection coefficient is complex, the reflected ground wave will differ in both amplitude and phase. The phase difference of the two paths is [14]

$$\Delta\varphi = \frac{2\pi}{\lambda}\{\sqrt{d^2 + (h_t + h_r)^2} - \sqrt{d^2 + (h_t - h_r)^2}\}. \tag{5}$$

If the field strength at the receiving antenna due to the direct line-of-sight wave is E_0, then the received field due to the sum of the direct line-of-sight component and ground reflected component is

$$E = E_0[1 + |\Gamma| exp(j\angle\Gamma - j\Delta\varphi)] = E_0[1 + |\Gamma|\cos(\angle\Gamma - \Delta\varphi) + j|\Gamma|\sin(\angle\Gamma - j\Delta\varphi)] \tag{6}$$

Taking the absolute value we find that

$$|E| = |E_0| [1 + |\Gamma|^2 + 2|\Gamma| \cos (\angle\Gamma - j\Delta\varphi)]^{1/2} \quad (7)$$

and since the received power p_r is proportional to the square of the received energy we have

$$p_r = |E_0|^2 [1 + |\Gamma|^2 + 2|\Gamma| \cos (\angle\Gamma - j\Delta\varphi)] \quad (8)$$

and

$$\frac{p_r}{p_t} = \left(\frac{\lambda}{4\pi d}\right)^2 G_t G_r [1 + |\Gamma|^2 + 2|\Gamma| \cos (\angle\Gamma - j\Delta\varphi)] . \quad (9)$$

If $d >> h_t h_r$, i.e. the angle of incidence becomes small, the reflection coefficient $\Gamma \rightarrow -1$. Thus (7) becomes

$$|E| = 2|E_0| \sin\frac{\Delta\varphi}{2} . \quad (10)$$

Then using the small angle approximation $\sin\Delta\varphi \approx \Delta\varphi$ and further expressing $\Delta\varphi \approx (4\pi h_t h_r) / (\lambda d)$, both valid approximations for a large separation distance, (9) can be expressed as

$$\frac{p_r}{p_t} = G_t G_r \left(\frac{4\pi h_t h_r}{d^2}\right)^2 . \quad (11)$$

3.3 Measurement Setup and Results

The experiments were primarily concerned with measurement of delay spread, Rician *K* factor and path loss versus distance; under various scenarios of automobile and antenna positions. The measurements were taken under stationary conditions on a roadway environment with parked cars. The antennas were supported by tripods at a height approximating an automobile's front hood. Two automobiles were parked in tandem at particular separation distance. As this distance was varied (from 6 to 40 feet), the parameters of interest were measured. At each distance, six measurements were taken at slightly different positions (by one half of the carrier wavelength to become uncorrelated) to average out fading.

The measurement setup consisted of four components as shown in Fig. 3.2. The com-

ponents are omnidirectional discone (receive and transmit) antennas, coaxial cables, a microwave network analyzer and a portable PC. The microwave network analyzer served as a signal generator and could cover a frequency range of 50 MHz to 13.5 GHz with a maximum frequency resolution of 100 kHz. The network analyzer automatically calibrated out the coaxial cable loss. All tests had a transmit power level of +10 dBm. The network analyzer provided frequency response as well as the time domain instantaneous impulse response data corresponding to a given frequency response sweep. This data was ported to the PC for analysis via a GPIB connection.

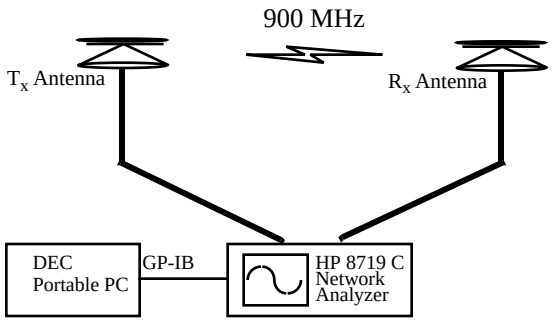

Figure 3.2 Measurement Setup

3.3.1 Path Loss Attenuation

Path loss rate was anticipated to be very close to, or perhaps slightly smaller than that of free space loss. As Fig. 3.3 shows, the measured rate was 2.36. A possible explanation for this somewhat large path loss value could be due to the inclusion of the measurement taken at the shortest distance. Indeed, with a carrier wavelength on the order of 1 foot in length (0.3333 meters to be exact), the short distance of 6 feet separating the two antennas comes somewhat close to the point at which antennas cease to act as "point sources": the antennas are clearly no longer in the far field. If this is the case, the path loss rate no longer follows the simple inverse square law. Indeed, when the path loss was calculated without the first point of Fig. 3.3, the new rate was 1.53. This question of being in the antennas far field was a pri-

mary reason for why measurements significantly closer (than 6 feet) were not taken.

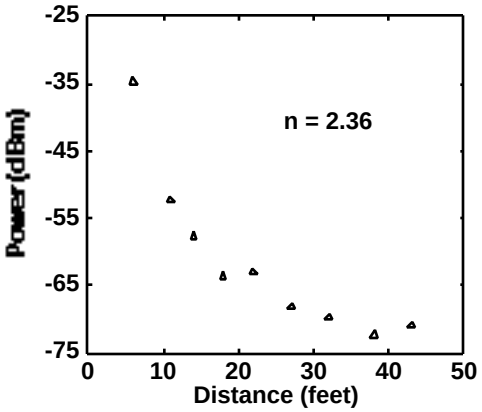

Figure 3.3 Path Loss

3.3.2 Delay Spread

Delay spread was measured using the technique presented in [15]. There are two interesting issues to note with the delay spread measurements in this experiment. First, the RMS delay spreads are, quite reasonably, very small. Compared to similar indoor wireless measurements that were have taken at 2.4 GHz with the same antenna separation distance, the vehicle to vehicle measurements have significantly smaller delay spreads (as much as a factor of 2). It is inferred that this difference is not due to the difference in carrier frequency but rather a difference in the two types of channel. One case being a relatively tame channel between two closely spaced automobiles, and the other being a relatively cluttered office cubicle environment. Given this difference, it seems quite reasonable that the vehicle to vehicle channel provides few obstacles that can lead to significant reflections, which is the primary cause of delay spreads.

A second interesting point is that the delay spread values increase slightly with distance but in a consistent oscillating pattern. As shown in Fig. 3.4, the RMS delay spread has an oscillating pattern and no four consecutive points can be connected by a monotonic curve. Referring to the concurrent indoor measurements done as part of this experiment as well as those of others [15, 18], it should be noted that this is uncharacteristic. Recall that

each data point in Fig. 3.4 represents six separate measurements taken within a small region to average out the effects of fading.

One explanation is the effect of a LOS path plus a ground reflection as the dominant components of the Rician channel model. One can view the channel as a phasor sum of: a) LOS, b) strong ground reflection, and c) many random scatters. The RMS delay spread tends to be inversely correlated with the amplitude of the two strong components. The oscillations in Fig. 3.4 diminish as distance increases. Beyond a certain turnover distance, the phasor sum of the two dominant phasor components no longer oscillate.

Another explanation could be that the relative received signal strength of "long" reflections in the channel oscillates as a function of antenna separation distance. The significant objects in our channel are simply two consecutive vehicles and a flat roadway. Furthermore, the test environment did not have any objects above the vehicles or to the left or right that were close enough to have a serious impact on the channel.

This observation has implications for many of the n-ray models (for integer n, typically small) that are being proposed to characterize channels. Models which describe a wireless channel as having a small, finite number of signal paths can afford an almost deterministic approach due to the reduced number of variables to consider. In effect, it may become possible to "predict" locations at which certain reflections may be cancelled out. It is this kind of prediction that would lend itself to explaining Fig. 3.4.

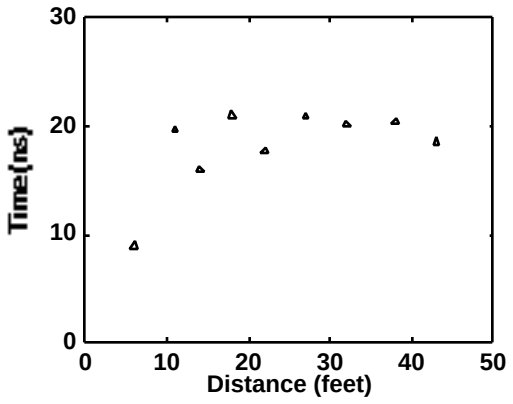

Figure 3.4 RMS Delay Spread vs. Antenna Separation Distance

3.3.3 Rician K Factor

The Rician *K* factor is very important in completing the knowledge about the associated probability density function of a wireless channel. Indeed, to know the distribution of a wireless channel without knowing the parameters about which the distribution occurs is useless. Knowledge of the Rician *K* Factor can be useful in determining the bit error rate of a channel among other useful metrics.

Note that the search for a Rician *K* factor implicitly suggests a Rician distribution has been assumed. Given the intuition that a Rician fading channel has a strong LOS component, this assumption is readily justified.

The method of moments was used to determine the Rician *K* factor. This method sets the sample mean equal to the theoretical mean (both of the received signal amplitude). The following equation shows the theoretical mean of a Rician distributed random variable.

$$E\rho = e^{-K/2}\sqrt{\frac{\pi}{2(K+1)}}\bar{p}\left[(1+K)\,I_0\left(\frac{K}{2}\right) + KI_1\left(\frac{K}{2}\right)\right] \tag{12}$$

Since both the local mean power, $\bar{p}$, and the sample mean, Eρ, are empirically determined, (12) can be used to solve for *K*.

The largest measured *K* factor was 17.6. This value occurred several times. More typical values were in the range of 5.0 to 11.0. Large *K* factors were anticipated due to the obvious strong LOS signal that is present between the two vehicles. Contrary to anticipation, however, were occasional measured *K* factors around 1.5 (the lowest was 1.38).

Recall that the *K* factor represents the ratio of the received LOS component to the received scattered components. This concept of *K* factor, first put forth in [13], is very difficult to measure in a physically meaningful manner; i.e., by isolating the direct signal from the scattered components. Since the *K* factor can serve as a metric for differentiating Rician from Rayleigh distributions, the question becomes, "how large must *K* be to truly have a Rician distribution?"

It is inferred that the consistency of larger measured *K* factors (i.e., 11.1, 17.6, etc.) is evidence of a Rician distribution. However, the few low values that were measured does cause concern. It seems more likely that the channel is Rician with a dominant component consisting of at least two paths; an LOS and a reflection off of the roadway. These two components may be interacting with one another in such a way as to have a sinusoidal type of frequency response which affects the computations.

As part of future work, alternative method for measuring the *K* factor can be employed. One, very nonexplicit method for accomplishing this task is to match various (with differing parameters) Rician distribution functions to the tabulated results from the measurements. The distribution (and corresponding *K* factor) that most closely matches is optimum.

3.4 Conclusion

The results of RF wireless vehicle to vehicle measurements at close range are: path loss with an exponential drop off rate of 2.36 and RMS delay spread with a range of values between 8.9 to 20.8 ns. Of note is the RMS delay spreads that had an "oscillating" behavior that can lend itself to many of the n-ray channel characterization models. Additionally, the Rician *K* factor results mostly range from 5.0 to 11.0 with extreme values as high as 17.6 and as low as 1.38. The channel is not strictly Rician. Unlike the traditional view of a Rician channel, it is inferred that the channel consists of two dominant components: a LOS signal and a strong reflection off of the roadway. Over distance the two dominant components sum up in a oscillatory manner.

3.5 References

[1] R.J.C. Bultitude and G.K. Bedal, "Propagation characteristics on microcellular urban radio channels at 910 MHz", *IEEE Jour. Sel. Areas in Commun.*, vol. 7, no. 1, 1989, pp. 31-39.

[2] D.C. Cox, "Multipath Delay Spread and Path Loss Correlation for 910-MHz Urban Mobile Radio Propagation", *IEEE Trans. Veh. Technol.*, vol. 26, no. 4, Nov. 1977, pp. 340-344.

[3] D.C. Cox and R.P. Leck, "Correlation bandwidth and delay spread multipath propagation statistics for 910-MHz urban mobile radio channels", *IEEE Trans.on Commun.*, vol. 23, no. 11, Nov. 1975, pp. 1271-80.

[4] D.C. Cox and R.P. Leck, "Distributions of multipath delay spread and average excess delay for 910-MHz urban mobile radio paths", *IEEE Trans.on Antennas and Propagation*, vol. 23, no.3, Mar. 1975, pp. 206-13.

[5] D.M.M. Devasirvatham, "Multipath time delay spread in the digital portable radio environment", *IEEE Commun. Mag.*, vol. 25, no. 6, June 1987, pp. 13 - 21.

[6] R. Ganesh and K. Pahlavan, "Effects of traffic and local movements on multipath characteristics of an indoor radio channel", *Electronics Letters*, vol. 26, no. 12, 7th June 1990, pp. 810 - 812.

[7] H. Hashemi, "The indoor radio propagation channel", *Proc. IEEE*, vol. 81, no. 7, July 1993, pp. 941 - 968.

[8] S. Howard and K. Pahlavan, "Doppler spread measurements of the indoor radio channel", *Electronics Letters*, vol. 26, no. 2, 1990, pp. 107-109.

[9] W.C. Jakes (Ed.), *Microwave Mobile Communications*, New York: Wiley, 1974.

[10] W.C.Y. Lee, *Mobile Communications Design Fundamentals*, Indianapolis: Sams, 1986.

[11] J.P.M.G. Linnartz, *Narrowband Land-Mobile Radio Networks*, Boston: Artech House, 1993.

[12] D. Molkdar, "Review on radio propagation into and within buildings", *IEE Proceedings-H*, vol. 138, no. 1, Feb. 1991, pp. 61-73.

[13] K.A. Norton, L.E. Vogler, W.V. Mansfield and P.J. Short, "The probability distribution of the amplitude of a constant vector plus a Rayleigh-distributed vector", *Proc. of the IRE*, Oct. 1955, pp. 1354-1361.

[14] J.D. Parsons, *The Mobile Radio Propagation Channel*, New York: Wiley, 1992.

[15] A. Polydoros, et al., *Vehicle to Roadside Communications Study*, PATH Research Report PRR-93-4, June 1993.

[16] J.G. Proakis, *Digital Communications*, 2nd ed., New York: McGraw-Hill, 1989.

[17] T.S. Rappaport, "Characterization of UHF multipath radio channels in factory buildings", *IEEE Trans. on Antennas and Propagation*, vol. 37, no. 8, Aug. 1989, pp. 1058 - 1069.

[18] A.M. Saleh and R.A. Valenzuela, "A statistical model for indoor multipath propagation", *IEEE J. Sel. Areas in Commun.*, vol. 5, no. 2, Feb. 1987, pp. 128-137.

[19] W.-C. Wong, "Packet reservation multiple access in a metropolitan microcellular radio environment", *IEEE J. Sel. Areas in Commun.*, vol. 11, no. 6, Aug. 1993.

[20] H. Harley, "Short distance attenuation measurements at 900 MHz and 1.8 GHz using

low antenna heights for microcells", *IEEE J. Sel. Areas in Commun.,* vol. 7, no. 1, 1989, pp. 5-10.

[21] J.P.M.G. Linnartz, "The modelling of diffraction, reflection, and clutter loss in UHF radio propagation", FEL-TNO report 1988-28, The Hague, The Netherlands, 1988.

[22] D.M.J. Devasirvatham, "Radio propagation studies in a small city for universal portable communications", *38th IEEE Veh. Technol. Conf.*, Philadelphia, PA, June 15-17, 1988, pp. 100-104.

[23] E.C. Jordan and K.G. Balmain, *Electromagnetic Waves and Radiating Systems*, New York: Prentice-Hall, 1968.

Chapter 4

Vehicle-to-Vehicle Communications for AVCS Platooning

As seen in previous chapters, vehicle-to-vehicle radio links suffer from multipath fading and interference from other vehicles. This chapter discusses the impact of these effects on communication networks supporting, in particular, AVCS. The statistical models for this channel are used to evaluate the performance of a network involving many links. The performance of Time Division Multiple Access (TDMA), Direct Sequence Code Division Multiple Access (DS-CDMA), and Frequency Hopping with TDMA in this environment are compared. Reliability of the radio link is investigated by specifying the radio spectrum occupation for a given required reliability of the radio link.

4.1 Introduction

In order to combat the effects of multipath fading and associated doppler shift as well as interference from other links multiple access schemes such as Time Division Multiple Access (TDMA), Direct Sequence Code Division Multiple Access (DS-CDMA), and Frequency Hopping with TDMA are investigated. Shladover [4] and Hitchcock [8] have shown that message delays within a platoon environment can have dire consequences. Thus the performance of these various multiple access schemes is quantified by Packet Erasure Rates (PER) as well as Reliability (probability of a successful message reception in a fixed time interval) for a given spectral allocation. Network protocol and frequency reuse in a platoon scenario will also be discussed.

Section 4.2 discusses the platoon model in which the communication links are located and the various elements that will affect the channel and communication link are highlighted. In Section 4.3 the channel model is described. Sections 4.4 and 4.5 deal with the modulation and multiple access schemes that are implemented in this channel. Section 4.6 discusses network protocol and frequency sharing procedures. In Section 4.7 the numerical results of the issues discussed in the preceding sections are formulated. Section 4.8 summarizes these results and draws conclusions and recommendations of this study.

4.2 Platoon Model

Shladover, et al., [4] have proposed a method of efficient vehicle control by grouping vehicles in platoons. "It requires electronically linked cars to travel in instrumented lanes with facilities to allow the vehicles to join and exit platoons smoothly at highway speeds. Estimates suggest that a [single automated lane] could carry as much traffic as three or four ordinary lanes. Platoons of up to four cars at speeds of 55 m.p.h. and up have already been tested and plans to test platoons of up to 20 cars are being implemented. It is possible to obtain very accurate lane holding (within 15 cm when under a variety of anomalous conditions) while maintaining excellent ride quality. Highway lanes could be much narrower

once automated. High-precision vehicle-follower control appears possible when dynamic data obtained by ranging sensors are combined with communication between cars." [3]

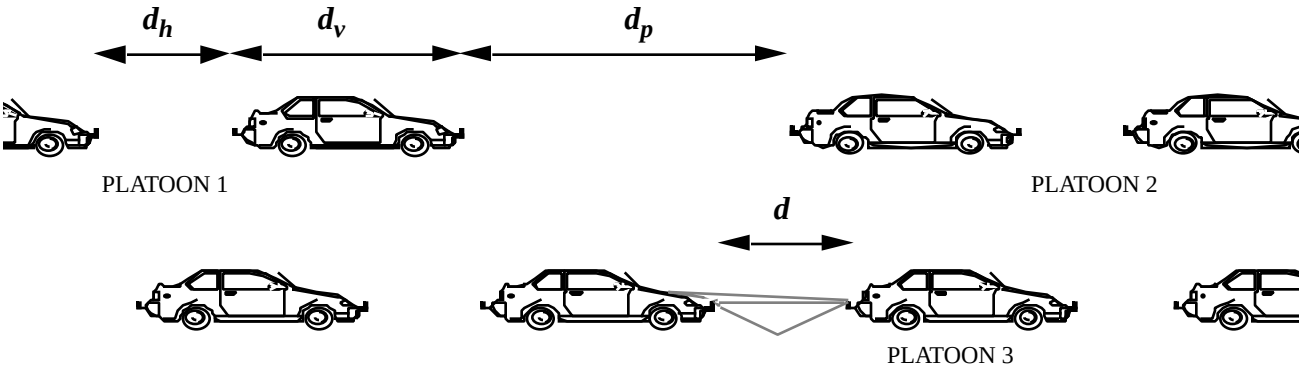

Figure 4.1 Platoon Model

We consider AVCS in a platoon environment, where a platoon consists of N vehicles. As depicted in Fig. 4.1, the distance between vehicles is denoted as d_h, and is on the order of 1 or 2 meters [4]. The vehicle length, platoon following distance, and lane width are denoted as d_v, d_p, and d_l respectively, while the communication link under study is denoted as d.

In slotted access cellular mobile transmission schemes different cells transmit over different frequencies in order to reduce interference. Frequency bands can be reused in cells spaced far enough apart such that the interfering energy between these cells is negligible. Each platoon, including the distance between the platoons, d_p, is considered a cell. Unlike most cellular radio schemes, the cells here are in relative motion with each other, since platoons in either lane may have a net difference in velocities. Thus we define two frequency reuse distances, d_r and d_s. The distance d_r is the reuse distance within a lane, whereas d_s is the reuse distance between lanes.

Thus for TDMA, if a cluster of C different frequencies is used, the frequency reuse distance within a lane is

$$d_r = C_r\,(d_p + (N-1)\,(d_v + d_h)) \tag{1}$$

whereas the reuse distance between lanes for both TDMA and CDMA is

$$d_s = C_s d_l. \tag{2}$$

Thus for TDMA $C = C_r C_s$ radio channels are required, each with bandwidth BT. Messages are of relatively short duration, typically a few hundreds of bits. The required transmission bandwidth is determined by the cycle duration T_c during which all vehicles in a platoon transmit their speed and acceleration data. Since CDMA transmission suppresses interference, successive platoons and platoons in other lanes may use the same channel.

4.3 Radio Channel Model

The RF propagation model in Chapter 3 is used. For large separation distances the local mean power approximately falls off according to an inverse fourth power law. From the analysis and empirical values reported for path loss in Chapter 3, the free-space loss dominates propagation between antennas of vehicles belonging to same platoon, where there may be a line-of-sight component ($d_i < N\,(d_v + d_h) << d_t$) and plane earth loss for interference signals propagating from one platoon to another, where the propagation distances are large. Therefore the n^{th} vehicle in a platoon receives an normalized interference signal with power $\bar{p}_m$ from the $m+n+1^{th}$ (for $m=1,2,3...$) vehicle given by

$$\bar{p}_m \approx m\,(d_v + d_h)^{-\beta_1} \tag{3}$$

and interference from two co-channel platoons with normalized power $\bar{p}_r$ given by

$$\bar{p}_r \approx d_r^{-(\beta_1 + \beta_2)}\, d_t^{-\beta_2} \quad . \tag{4}$$

In a dispersive Rician fading channel, energy arrives at the transmitter from reflections as well as a dominant wave, which we define as the phasor sum of a direct line-of-sight wave and a strong ground reflected wave. Thus the received signal of the i^{th} vehicle is in the form

$$\nu_i(t) = c_0 \cos\left(\omega_c t + \Phi_0 + \psi_i(t)\right) + \sum_{k=1}^{K} c_k \cos\left(\omega_c t + \Phi_k + \psi\left(t - T_k\right)\right) \quad , \tag{5}$$

where the constant c_0 represents the amplitude of the dominant component, as found in (7), and Φ_0 the phase delay in the dominant component. The variables c_k, Φ_k and T_k represent the amplitudes, phases and delay times of the k^{th} reflected wave (k = 1, 2,....,K). Digital phase modulation is incorporated in $\psi_i(t)$. The reflections $\{k: T_k < T_b\}$ are assumed to add coherently to the dominant component and along with the dominant component make up the first resolvable Rician path. The remaining reflections cause intersymbol interference.

We define the Rician parameter K_1 as the ratio of the power $\bar{p}_0$ in the dominant component to the local-mean scattered power $\bar{p}_1$ in the first resolvable path. The Rician parameter K_2 is defined as the ratio of the power $\bar{p}_0$ in the direct line-of-sight component to the excessively delayed local-mean scattered power $\bar{p}_2$. The local-mean power $\bar{p}$ is the sum of the power in the dominant component and the average powers in the scattered components ($\bar{p} = \bar{p}_0 + \bar{p}_1 + \bar{p}_2$). The Rician K factor, defined as the ratio of the power in the dominant component to the total scattered power is

$$K = \left(\frac{1}{K_1} + \frac{1}{K_2} \right)^{-1}. \tag{6}$$

Since the local mean power of the dominant component varies with distance, as shown in the previous section, the above Rician parameters, although not stated explicitly, are also functions of distance.

This channel behaves as a narrowband Rician-fading channel with Rayleigh distributed intersymbol interference. For m = 0,1, or 2 and $K_0 = 1$,

$$c_0^2 = 2\bar{p}_0 = \frac{2\bar{p}K}{1+K} \tag{7}$$

$$\overline{p_m} = \frac{\bar{p}K}{K_m(1+K)} \quad . \tag{8}$$

In the following, K is assumed to be determined by the propagation environment and path length. The relative values of K_1 and K_2 are determined by the delay profile and the

symbol rate. The probability distribution function of the signal amplitude, expressed in terms of the local-mean power $\bar{p}$ and the Rician K-factor becomes

$$f_\rho\langle\rho|\bar{p}, K\rangle = \frac{\rho(1+K)}{\bar{p}KK_1}e^{-K_1}exp\left(-\frac{\rho^2(1+K)}{2\bar{p}KK_1}\right)I_0\left(\rho K_1\sqrt{\frac{2(1+K)}{\bar{p}K}}\right) \tag{9}$$

and thus for the instantaneous power we have

$$f_p\langle p|\bar{p}, K\rangle = \frac{(1+K)}{2\bar{p}KK_1}e^{-K_1}exp\left(-\frac{p(1+K)}{\bar{p}KK_1}\right)I_0\left(2K_1\sqrt{\frac{p(1+K)}{\bar{p}K}}\right) \quad . \tag{10}$$

For interfering signals, the propagation distance is significantly larger, and because of the relatively low antenna height, a line-of-sight component may not be present. In such cases, Rayleigh fading (Complex Gaussian) appears a reasonable model.

4.4 Modulation Scheme

The ideal bit error rate for BPSK modulation in a time-invariant AWGN channel is [14]:

$$P_b(e) = \frac{1}{2}erfc\sqrt{E_b/N_0} \quad , \tag{11}$$

where N_0 is the (one-sided) spectral power density of the AWGN, E_b is the constant received energy per bit $(E_b = p_0T_b)$ and erfc(.) denotes the complementary error function [15]. The in-phase component of Rayleigh fading co-channel interference may be approximated as Gaussian noise, giving a mean error probability of [10]

$$P_b(e|\rho, \bar{p}_r, \bar{p}_2) = \frac{1}{2}erfc\left(\sqrt{\frac{\frac{1}{2}\rho^2T_b}{\bar{p}_rT_b + \bar{p}_2T_b + N_0}}\right) \quad , \tag{12}$$

An approximation often used for the probability of bit error in CDMA is

$$P_b\langle e|\rho, \bar{p}_t, \bar{p}_2\rangle = \frac{1}{2}erfc\sqrt{\frac{\frac{1}{2}\rho^2T_b}{\frac{(C_s\bar{p}_tT_b + \bar{p}_2T_b)}{N} + N_0}} \tag{13}$$

where N is the spreading gain of the CDMA scheme and C_s is the frequency reuse factor between lanes. The average BER can then be found by integrating over the Rician pdf of the signal amplitude given in (9)

$$\overline{p_b} = \int_0^{\infty} \frac{\rho(1+K)}{\bar{p}KK_1} e^{-K_1} exp\left(-\frac{\rho^2(1+K)}{2\bar{p}KK_1}\right) I_0\left(\rho K_1 \sqrt{\frac{2(1+K)}{\bar{p}K}}\right) \times P_b\langle e|\rho, p_r, p_2\rangle d\rho \quad . \quad (14)$$

4.5 Multiple Access Schemes

In this section we compare TDMA, TDMA with slow frequency hopping interferers, and Direct Sequence CDMA (DS-CDMA) with regards to Packet Erasure Rates (PER). We use spreading mainly to suppress interference. In other applications the frequency diversity of CDMA is also exploited. However the delay spread is too small. Dynamic power control cannot be easily used as mulitple receivers.

4.5.1 Packet Erasure Rates

A packet erasure occurs when bit errors are in excess of the correcting capabilities of the error correction coding being implemented. Slow and fast Rician fading of the wanted signal are considered with a block error detection code that can correct up to M errors in a block of L bits.

With fast fading, the duration of the packets is substantially longer than the time constants of the multipath fading. This is the case with continuous wave CDMA transmission with a bit rate of 5 kbps and a carrier frequency of 1 GHz and vehicle speed of 30 m/s (~70 miles/hour). The received signal experiences several fades during packet transmission. We assume that during one bit time, the channel characteristics do not change, but that the received amplitude are statistically independent from bit to bit, even though the receiver remains perfectly locked to the wanted signal. So the probability of undetected packet errors for BPSK is obtained from

$$P\langle e|\bar{p}_o, \bar{p}_r\rangle = 1 - \sum_{m=0}^{M} \binom{L}{m} (1-\overline{p}_b)^{L-m} (\overline{p}_b)^m \quad (15)$$

where the average bit error probability $\overline{p}_b$ is defined in (14).

Slow fading occurs when packets are of sufficiently short duration, that the received amplitude and carrier phase may be assumed to be constant throughout the duration of the packet. This condition is satisfied if the motion of the mobile terminal during the transmission time of a block of bits is negligible compare to the wavelength. This is the case with TDMA transmission at a rate above 100 kbps to accomodate user bit rates of 5 kbps with an average frame of 20 cars per platoon. The probability of packet erasure in a block of L bits with M bit correction is found by averaging the probability of packet error over the Rician fading of the wanted signal. In our case,

$$P\langle e|\bar{p}_o, \bar{p}_t\rangle = \int_0^{\infty} \frac{(1+K)}{2pKK_1} e^{-K_1} exp\left(-\frac{p(1+K)}{\bar{p}KK_1}\right) I_0\left(2K_1\sqrt{\frac{p(1+K)}{pK}}\right)$$

$$\times \left\{1 - \sum_{m=0}^{M} \binom{L}{m}\left(1 - \frac{1}{2}erfc\left(\sqrt{\frac{pT_b}{\bar{p}_r T_b + \bar{p}_2 T_b + N_0}}\right)\right)^{L-m}\left(\frac{1}{2}erfc\left(\sqrt{\frac{pT_b}{\bar{p}_r T_b + \bar{p}_2 T_b + N_0}}\right)\right)^m\right\} dp \quad (16)$$

4.6 Network Protocol

Our TDMA radio protocol is as follows: the lead vehicle transmits a message containing speed and acceleration to the second vehicle, upon reception of a report by the n^{th} vehicle, the n^{th} vehicle sends its report. The performance of the radio link can be quantified by the probability that a message can be successfully transmitted across a platoon from one vehicle to another. We define the completion of a message through a platoon in this manner as a cycle. If a vehicle does not recognize a message or erroneously detects a message, the cycle is interrupted. To ensure safe operation of the AVCS vehicle control system, we require a very small probability of undetected errors. On the other hand we wish a large probability

that a cycle is completed successfully. The n^{th} vehicle transmits its report after it has successively received messages with bit pattern which differed in less than M_2 places from a valid codeword of the $n\text{-}1^{th}$ vehicle. A message is assumed to be received successfully and reliably if the detected bit sequences does not differ in more than M_1 places from a valid code word. It is not necessary to take $M_1 = M_2$. In fact if $M_1 < M_2$, the terminal may transmit its own status assuming that it's turn to transmit has arrived, yet not entirely relying upon the data in the received packet because of a large number of bit errors. The performance of the network is quantified by finding the probability that the $(n\text{-}1)^{th}$ vehicle successfully transmits its report to the n^{th} vehicle, with $M_1 < M_2$. In an AVCS environment the lead vehicle generates data that all vehicles in the platoon require[4], thus we are also interested in the probability that the lead vehicle successfully transmits its report to the n^{th} vehicle, this occurs if each hop has less than M_1 bit errors.

4.7 Numerical Results

The length of each vehicle, $d_{v,}$ was assumed to be 5 meters; the lane width, d_l, 3 meters; the distance between automated cars, d_h, 1 meter; and the average velocity of an automated vehicle was assumed to be 70 m.p.h. The distance of the radio link under study, d, was varied from 0.1meterstо10meters. From Chapter 3, $K = 7dB$ $(K_1 \approx 5)$ is reasonable for most vehicle-to-vehicle channels, $K_1 = 10$ is assumed as an upper bound. All vehicles transmit data with the same power. The signal to noise (AWGN Gaussian) ratio was set to 10 dB at a distance of $d = 10$ meters.

The radio link suffers from interference from within its platoon (P_1), from platoons in the same lane (P_2), and co-channel interference from platoons in other lanes (P_3 and P_4). In all simulations we assume that the target vehicle is joining an infinitely long platoon. It should be noted that in TDMA transmission each vehicle within a platoon is given a time slot in which to transmit, thus P_1 will be zero; while for CDMA type transmission all vehicles transmit at the same time, thus P_1 must be taken into account. We assume P_2 is negligi-

ble since transmissions from other platoons must be reflected off vehicles, road surface, and surroundings before reaching the receiver. These reflections will greatly attenuate the signal. We thus set $d_r = C_r = 0$ in (2) . To obtain an upper bound on the P_3 and P_4 we assume that an infinitely long platoon would transmit as close as possible to the receiving vehicle. Lacking accurate measurements, it was assumed that these signals would attenuate by10 dB for each lane traversed, thus P_4 would be 10 dB less than P_3.

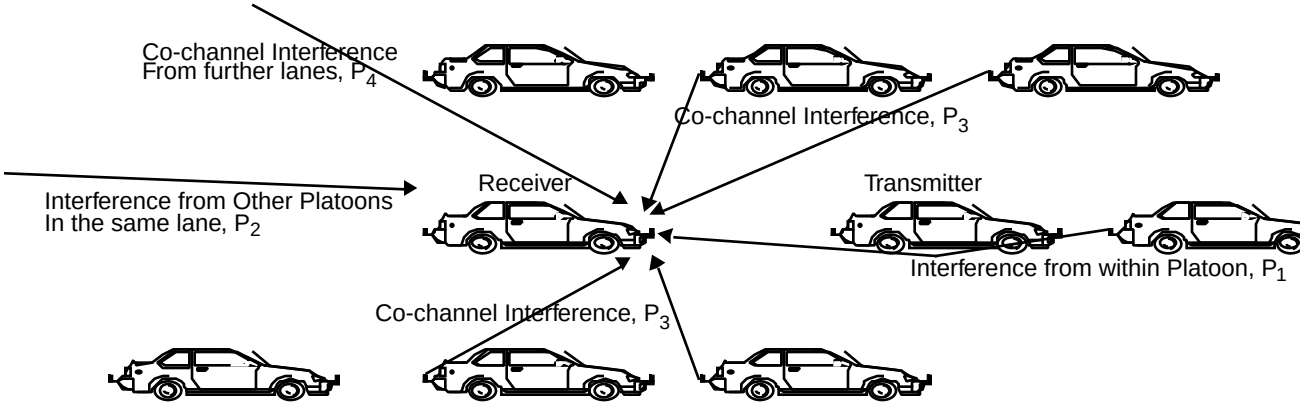

Figure 4.2 Assumptions about Interference in radio link

4.7.1 Bit error rates

We will first show bit error rates (BER) as a function of distance as described in (12)-(14) and compare them to a channel model in which a strongly reflected ground wave is not present.

Fig. 4.3 examines the effect of varying the reuse pattern C_r for CDMA transmission employing horizontal polarization or vertical polarization. For $N = 32$, the bit error rates show a great change only when $C_r = 1$. For other curves (not plotted here) it appeared that for a reuse pattern is greater than one or two and $N > 32$ the bit error rates remain relatively the same, independent of spreading factor and reuse pattern. We will concentrate on CDMA

with a reuse factor $C_r = 2$ and a spreading factor $N = 32$, since this will give nearly the same performance as other schemes, but with minimal bandwidth.

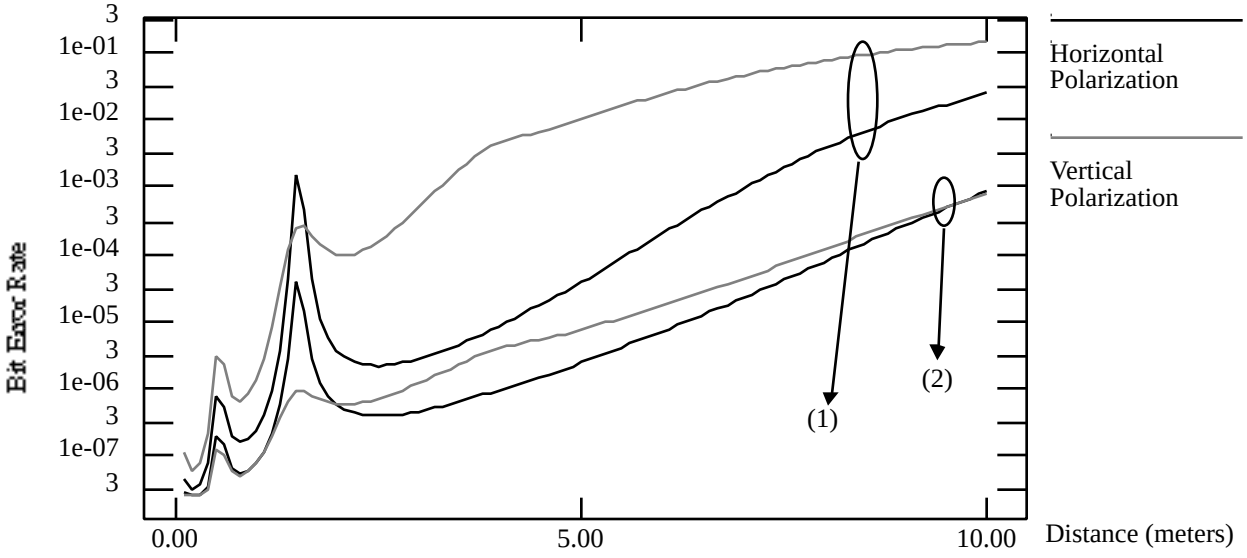

Figure 4.3 Bit error rates for CDMA: $N = 32$ with vertical and horizontal polarization. (1) $C_r = 1$ (2) $C_r = 2$.

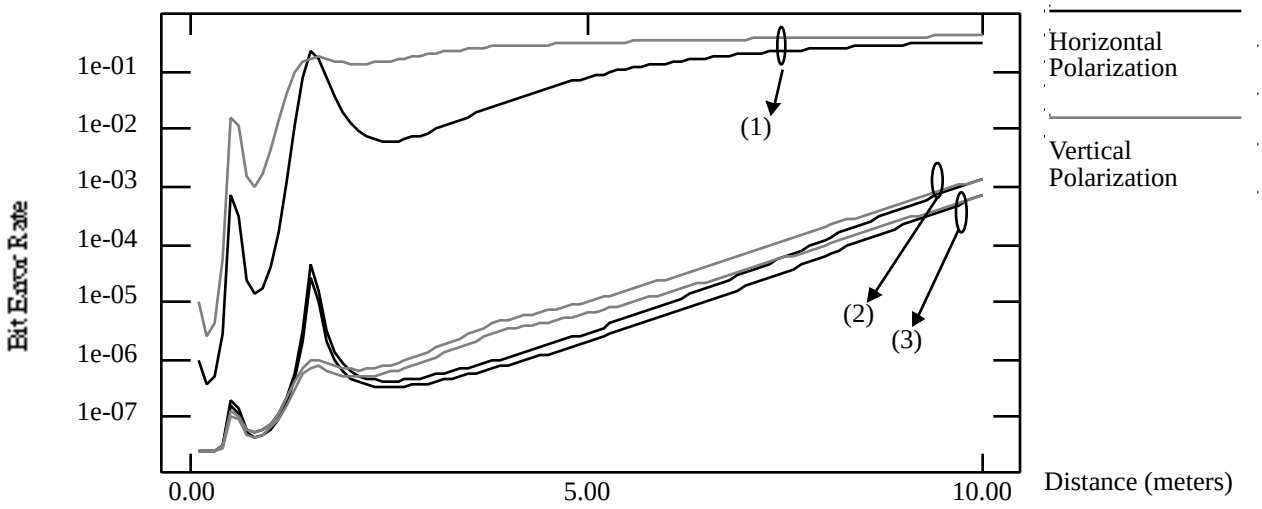

Figure 4.4 Bit error rates for TDMA with vertical and horizontal polarization. (1) $C_r = 1$ (2) $C_r = 2$. (3) $C_r = 6$.

The effects of varying frequency reuse patterns for TDMA is presented in Fig. 4.4. Here we see that unlike the CDMA case varying the reuse pattern has a significant impact on the bit error rates, thus TDMA is more sensitive to interference than CDMA. However as C_r

increases the gain in performance decreases. So by using more bandwidth (increasing C_r) we get smaller and smaller gain in performance (lower BER). We will concentrate on TDMA with a reuse pattern of $C_r = 3$.

4.7.2 Packet Erasure Rates

As explained in Section 4.5 the assumptions were a fast fading channel for CDMA and a slow fading channel for TDMA. We also assume a packet length of $L = 76$ bits with one bit correction ($M_1 = 1$) [34]. Fig. 4.5 compares TDMA and CDMA packet erasure rates with horizontal polarization. It should be noted that these system require different bandwidths. Although the bit error rates for TDMA with $C_r = 3$ and CDMA with $C_r = 2$, $N = 32$ were nearly identical, the packet error rates for the same situation differs significantly. In order to increase the performance of TDMA one can use Slow Frequency Hopping within each platoon a TDMA type polling scheme is implemented. However a different carrier frequency for each platoon is chosen, according to a pseudo-random hopping sequence, at the end of every packet reception. Thus from Fig. 4.3, the co-channel interference power P_3 and P_4 are reduced since there is a large probability that adjacent lanes use different carrier frequencies. For a reuse pattern C_r=2, two independent sets of hopping frequencies (H) are used. A reuse factor of C_r=3 and a set of H=10 hopping frequencies outperforms CDMA and TDMA.

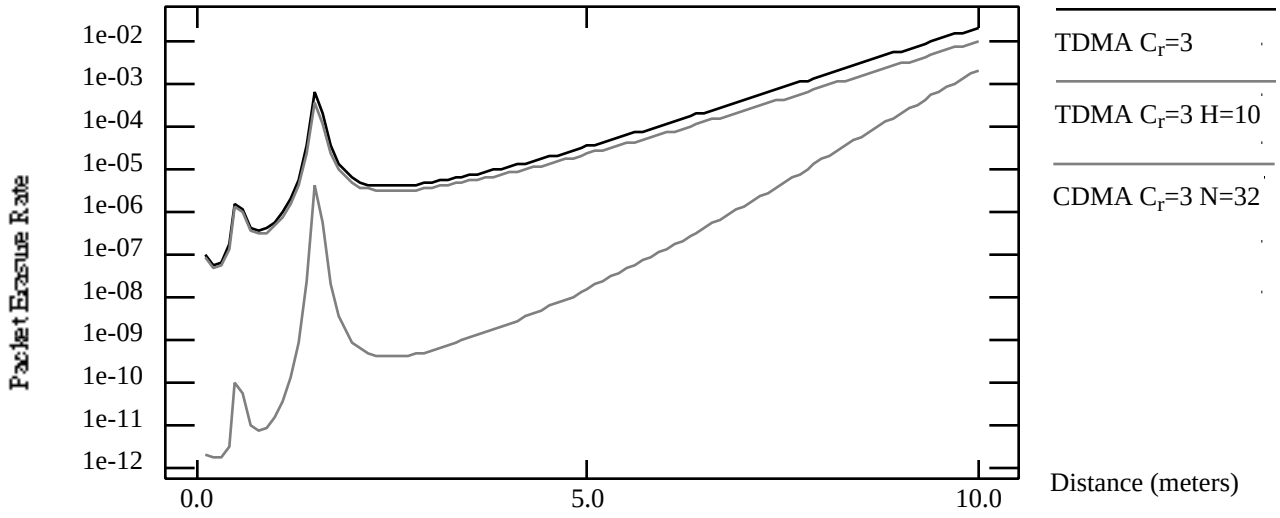

Figure 4.5 Comparison of CDMA, TDMA, and slow frequency hopping.

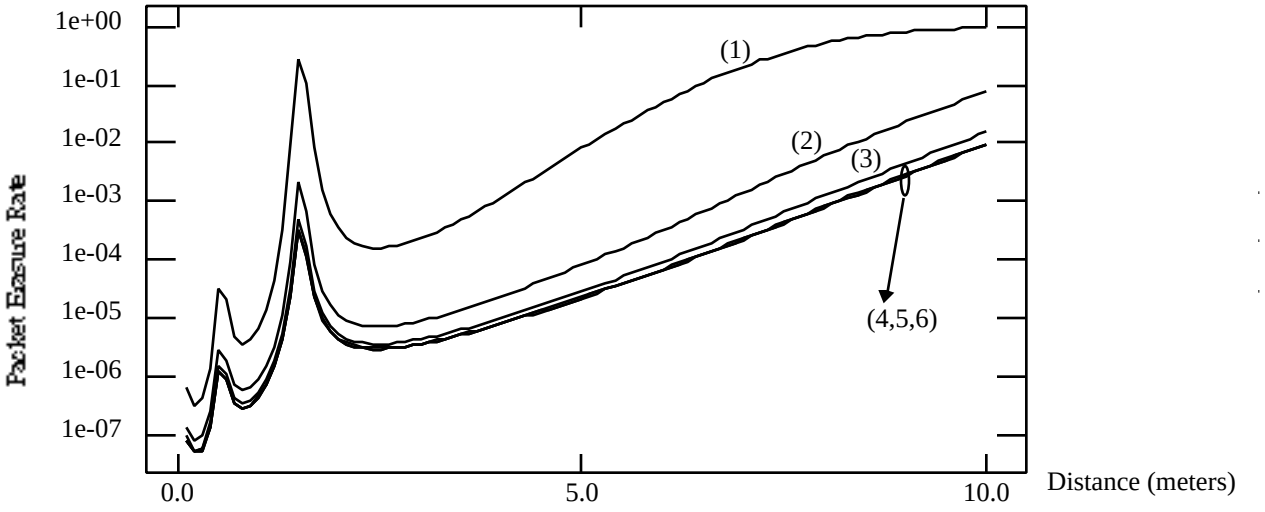

Figure 4.6 TDMA with slow frequency hopping for various reuse factors (C_r) and Hopping Frequencies (H). (1) C_r=1 H=10 (2) C_r=1 H=100 (3) C_r=2 H=10 (4) C_r=2 H=100 (5) C_r=3 H=10 (6) C_r=3 H=100.

Fig. 4.7 shows that vertical polarization yields better results for distances less than three meters and slightly higher packet erasure rates for distances greater than three meters.

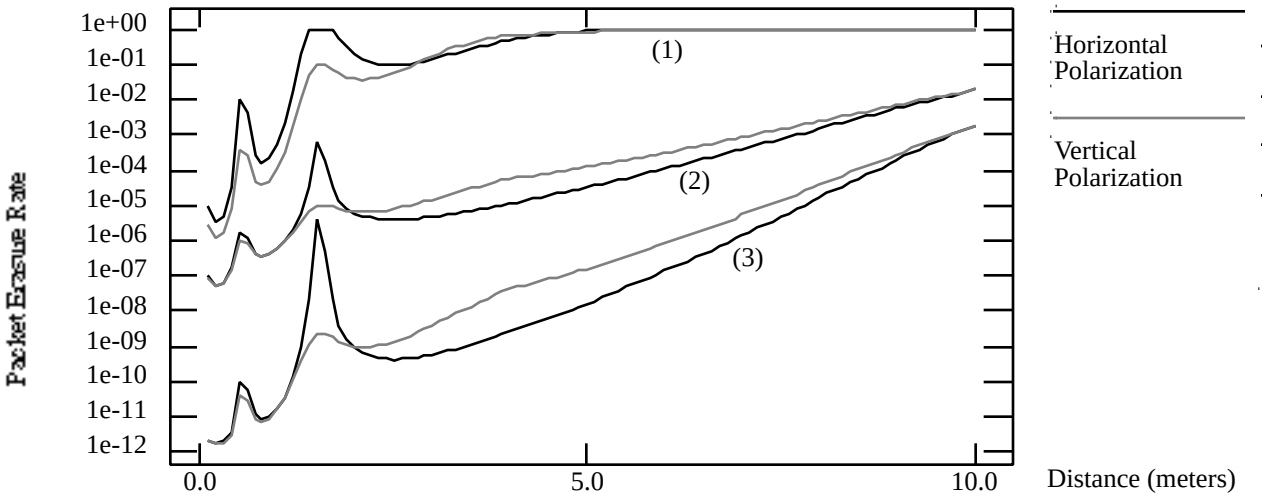

Figure 4.7 Comparison of TDMA and CDMA packet erasre rates for horizontal and vertical polarization. (1) TDMA C_r=1 (2) TDMA C_r=3 (3) CDMA C_r=2 N=32.

4.7.3 Reliability and Spectrum Allocation

This section quantifies the different bandwidth requirements of the previous schemes by presenting numerical analysis results of Reliability vs. Spectrum Allocation. Reliability *R(T,d)* is defined as the probability no message passes through our communication link in time *T* when the vehicles are at a distance *d*. For AVCS, it is relevant that updates arrive at least once every 50 msec, or so. We chose *T* = 50 msec and call T (as other sources also refer to this) as the deadline failure probability. In our results we have assumed a maximum *T=50 msec* at a link distance *d=10m* [4].

*A*lthough CDMA C_r=2, *N*=32 gives better PER results than TDMA, it requires much more bandwidth. Thus we can implement TDMA by requiring very frequent transmissions and though many of these transmissions would be lost, we are guaranteed a successful transmission using less bandwidth than CDMA. The gain in PER by frequency hopping also came as a result of greater bandwidth requirements, although not as much as CDMA. Interestingly TDMA C_r=*3* requires less bandwidth for a given reliability than TDMA C_r=*2*, since even though TDMA C_r=*3* requires more frequency bands per lane, the gain in PER is large enough that fewer transmissions are required. We see that this in not true for frequency hopping.

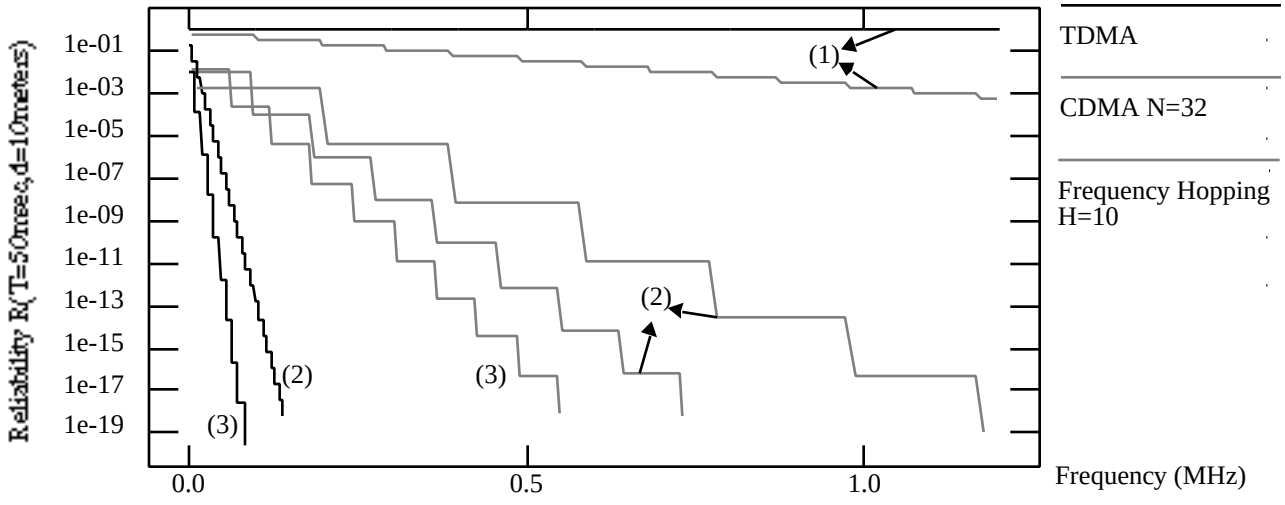

Figure 4.8 Reliability vs. Spectrum allocation for CDMA, TDMA, frequency hopping. (1) C_r=1 (2) C_r=2 (3) C_r=3.

4.7.4 Network Protocol

The preceding section described a network protocol for TDMA transmissions. The concept of a complete cycle through a platoon was developed and the idea propounded that the cycle sequence could be maintained without retransmission even though the received codeword differed from a valid code word by more than the distance accepted for error correction. Again employing the assumptions of the previous sections, it is shown how variations in M_1 (correcting distance used) and M_2 (error distance accepted for sync) affect the probability of cycle completion for both TDMA and frequency hopping.

Fig. 4.9 illustrates this. The probability of successful transmission between two links, requires all links to have less than M_1 errors. While the solid lines apply for only the link between $n\text{-}1^{th}$ and n^{th} vehicle which needs to have less than M_1 errors, while the n-2 prior links need only to have less than M_2 errors. Thus for TDMA it is critical that a cycle be maintained. While for CDMA all vehicles transmit simultaneously, thus preservation of the cycle is not as important.

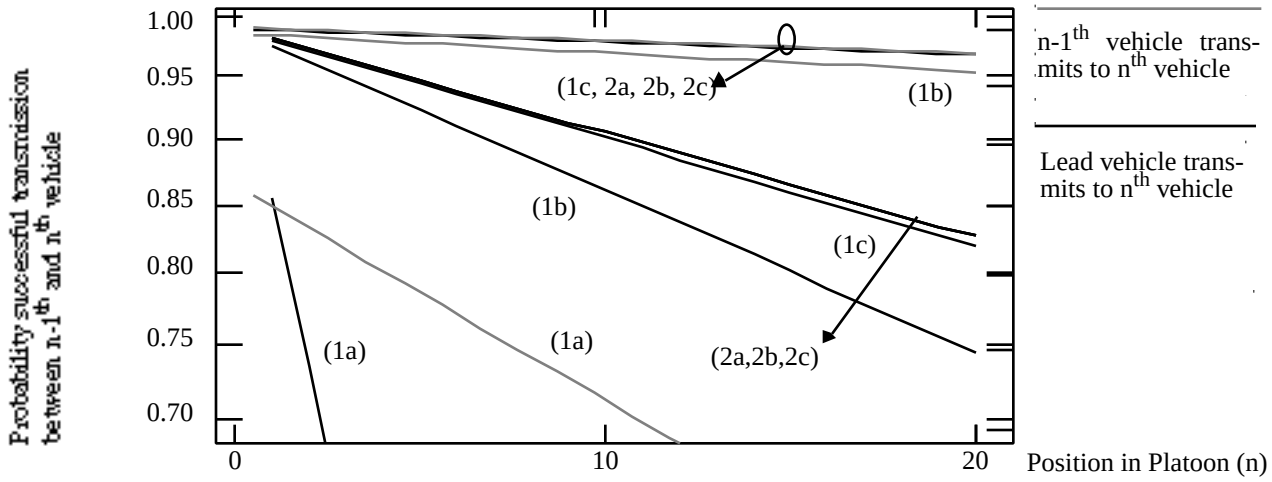

Figure 4.9 Probability of one vehicle in platoon transmitting to another vs. position in platoon. M_1=M_2=1, L=76, d_h=10m. (1) C=3 (2) C=6 (a) H=1 (b) H=10 (c) H=100

4.8 Conclusions

The statistical model developed in Chapters 2 and 3 for vehicle-to-vehicle radio channel applicable to AVCS communication was used, and extended, taking into account a dominant wave composed of a direct line-of-sight wave with a strongly ground reflected wave. The performance of this radio link was gauged by bit error rates, packet erasure rates, and deadline failure probability for a given bandwidth. These parameters were evaluated for three multiple access techniques: Time Division Multiple Access, (Direct Sequence) Code Division Multiplexing Access, and Time Division Multiple Access within a platoon with Frequency Hopping outside the platoon.

Our analysis showed that deep fades and large probability of packet loss can occur for distances less than three meters, due to the cancellation of the ground reflected wave and the direct line-of-sight wave. The effects of these fades could be reduced by employing vertical polarization as opposed to horizontal polarization. However for distance greater than three meters, horizontal polarization PER and BER performance showed an improvement over vertical polarization. The performance difference between polarization techniques for distances greater than three meters could be mitigated by decreasing co-channel interference (increasing the frequency reuse pattern thus increasing bandwidth). Thus if frequency reuse between lanes is employed, vertical polarization can be implemented in order to mitigate the effects of deep fades caused by the destructive interference between the ground reflected wave and the direct line-of-sight wave. Antenna diversity can also be used to increase performance [12].

The system under study was also found to be sensitive to co-channel interference. Our analysis showed that even for CDMA transmission, performance could be largely improved if adjacent lanes use different frequencies. However, increasing the reuse factor greater than two, for CDMA, and three, for TDMA, did not afford better performance. According to our computations and within the validity of our assumptions, CDMA provides lower packet erasure probabilities than TDMA or slow frequency hopping. However for a fixed band-

width system, the reliability for a given bandwidth or delay line failure probability appears to be better with TDMA. Here we see a trade off between error probabilities and bandwidth. With CDMA increasing bandwidth results in lower error rates. However with TDMA even though the error rates may be greater than CDMA, many transmissions are possible since the bandwidth requirements of TDMA are minimal compared to CDMA. TDMA also affords the system designer to implement a protocol scheme in which correct packet reception is not necessary in order to transmit an update to the next vehicle. As our analysis showed by varying the allowable number of bit errors in a received packet the delay in a TDMA system can further be reduced.

4.9 References

[1] K. Takada, Y. Tanaka, A. Igarashi, and D. Fujita, "Road/Automobile Communication System and its economic effect", *IEEE Vehicle Navigation and Information System Conf.*, pp. A15-21, 1989.

[2] I. Catling and P. Belcher, "Autoguide - goute guidance in the United Kingdom", *IEEE Vehicle Navigation and Information System Conf.*, pp. 467-473, 1989.

[3] W.C. Collier and R.J. Weiland, "Smart cars, smart highways", *IEEE Spectrum*, pp. 27-33, Apr. 1994.

[4] S. E. Shladover, et al., "Automatic vehicle control developments in the PATH Program," *IEEE Trans. Veh. Technol.*, vol. 40, no. 1, Feb. 1991, pp. 114-130.

[5] W.C. Jakes (Ed.), *Microwave Mobile Communication*, New York: Wiley, 1974.

[6] R.H. Clarke, "A Statistical Theory of Mobile Radio Reception", *Bell. Syst. Tech. J.*, July 1968, pp. 957-1000.

[7] A.S. Akki and F. Haber, "A statistical model of mobile to mobile land communication channel," *IEEE Trans. Veh. Technol.*,vol. 35, no. 1, 1986, pp. 2-7.

[8] A. Hitchcock, "An example of quantative evaluation of AVCS safety", *Pacific Rim TransTech Conference: Proceedings*, vol. I, Seatle, 1993, pp. 380-386.

[9] S.E. Ijaha, "Characterization of short-range microwave radio transponding channels for road-use debiting schemes", *6th Int. Conf on Mobile Radio and Personal Communications*, Warwick, Dec. 1991, pp. 261-266.

[10] J.P.M G. Linnartz, *Narrowband Land-Mobile Radio Networks*, Boston: Artech House, 1993.

[11] H. Harley, "Short distance attenuation measurements at 900 MHz and 1.8 GHz using low antenna heights for microcells," *IEEE J. Sel. Areas in Commun.*, vol. 7, no. 1, pp. 5-10, 1989.

[12] D. Parsons, *The Mobile Radio Propagation Channel*, New York: Wiley, 1992.

[13] E. C.Jordan and K.G. Balmain, *Electromagnetic Waves and Radiating Systems*, New York: Prentice-Hall, 1968.

[14] J.G. Proakis, *Digital Communications*, 2nd ed., New York: McGraw-Hill, 1989.

[15] M. Abramowitz and I.A. Stegun, *Handbook of Mathematical Functions*, New York: Dover, 1974.

[16] I.M.I. Habbab, M. Kahvehrad and C.E.W. Sundberg, "ALOHA with capture over slow and fast fading channels with coding and diversity," *IEEE J. Sel. Areas in Commun.*, vol. 7, no. 1, Jan. 1989, pp. 79-88.

[17] K. Zang, K. Pahlavan and R. Ganesh, "Slotted ALOHA networks with PSK modulation in Rayleigh fading channels", *Electron Lett.*,vol. 23, no. 6, 16th March 1989, pp. 413-414.

[18] J.P.M.G. Linnartz, H. Goosen, and R. Hekmat, "Comment on 'Slotted ALOHA radio networks with PSK modulation in Rayleigh fading channels'", *Electron. Lett.*, vol. 26, no. 9, 26th April 1990, pp. 593-595.

[19] W. R. Bennet, "Distribution of the sum of randomly phased components," *Quart. Appl. Math*., pp. 385-395, vol. 5, 1948.

[20] S. Gradshteyn and I.M. Ryzhik, *Tables of Integrals, Series and Products*, New York: Academic Press, 1965.

[21] S.O. Rice, "Statistical properties of sine wave plus random noise", *Bell Syst. Tech. J.*, pp. 292-332, Jan. 1948.

[22] F. Bowman, *Introduction to Bessel Functions*, New York: Dover, 1958.

[23] A. Leon-Garcia, *Probability and Random Processes for Electrical Engineering*, New York: Addison-Wesley, 1989.

[24] T. Aulin, "A modified model for the fading signal at a mobile radio channel", *IEEE Trans. Veh. Technol.* ,vol. 28, no. 3, 1979, pp. 182-203.

[25] W.B. Davenport and W.L. Root, *An Introduction to the Theory of Random Signals and Noise*, New York: McGraw-Hill, 1958.

[26] A. Aghamohammadi and H. Meyr, "On the error probability of linearly modulated signals in Rayleigh frequency-flat fading channels", *IEEE Trans. on Commun.*, vol. 38, no. 11, Nov. 1990, pp.1966-1970.

[27] R. Steele and V.K. Prabhu, "High-user-density digital cellular mobile radio systems", *IEE Proceedings F*, vol. 132, no. 5, Aug. 1985, pp. 396- 404.

[28] I. Porch, "Communication protocols to implement coordinated maneuvers of automatically controlled vehicles", EECS Dept., University of California at Berkeley, March 2, 1992.

[29] O. Shimbo and R. Feng, "Effects of co-channel interference and Gaussian noise in M-ary PSK system", *COMSAT Tech. Rev.*, vol. 3, no. 1, Spring 1973, pp. 183-207.

[30] K.H.H. Wong and R. Steele, "Transmission of digital speech in highway microcells", *Journal of the Inst. of Electronic and Electrical Eng.*, vol. 57, no.6 (supplement), Nov./Dec. 1987, pp. s246-s254.

[31] E.F. Casas and C. Leung, "OFDM for data communication over mobile radio FM channels - Part I: Analysis and experimental results," *IEEE Trans. on Commun.*, vol. 39, May 1991, pp. 783-793.

[32] R.J.C. Bultitude and G.K. Bedal, "Propagation characteristics on microcellular urban radio channels at 910 MHz", *IEEE J. Sel. Areas in Commun.*, vol. 7, no. 1, 1989, pp. 31-39.

[33] A.L. Maffett, *Topics for a Statistical Description of Radar Cross Section*, New York: Wiley, 1989.

[34] J.P.M.G. Linnartz and J. Walrand, *Spectrum Needs for IVHS*, PATH working paper UCB-ITS-PPWP-93-13, Sept. 1993.

Chapter 5

Base Station to Vehicle Communication

This chapter addresses roadside-to-vehicle communication via radio channels. The access schemes and the radio transmission techniques have to be designed in order to minimize the adverse effects of Rician multipath reception. The limited availability of bandwidth and the need to accommodate the foreseen traffic make co-channel interference another important factor. Vehicle-to-base station communication involves initial competition for access to the base station. Once access to the station is secured a short communication session in which data is exchanged will follow. Each base stations, on the other hand, may schedule transmissions to its vehicles avoiding conflits, but in some implementations different base station may transmit independently of other co-channel stations. This chapter is concerned with the design, analysis, and computation of results for transmission across the physical channel, as well as specifying requirements to optimize spectral efficiency on the link between roadside stations and the vehicles. An optimum frequency reuse factor of 2 is proposed to maximize network throughput, and to minimize average queueing delays. We hence find that frequency reuse can be substantially more dense than is acceptable for cellular telephony networks.

5.1 Introduction

This chapter is concerned with the design, analysis, and computation of results for transmission across the physical channel, as well as specifying requirements to optimize spectral efficiency on the link between roadside stations and the vehicles. An optimum frequency reuse factor will be proposed to maximize network throughput and to minimize average queueing delays: the frequency reuse can be substantially more dense than is acceptable for cellular telephony networks. Studies on the communication requirements [17] for the link between vehicles and base stations indicate that generally, throughputs on the order of 5 to 80 kbps per cell are acceptable for the uplink, and more than sufficient for the downlink in Automated Vehicle Control Systems (AVCS). Also, frame sizes of 77 to 130 bits are typical, and delays on the order of a few seconds are acceptable for AVCS. In this chapter these parameters are used to study the performance of the roadside base station to vehicle link, with the physical limitations of the short-range highway propagation environment also being accounted for. Frequency reuse and antenna directionality are investigated in an effort to optimize spectrum efficiency and queueing performance at the base stations.

Section 5.2 describes the parameters of that were considered in this study.

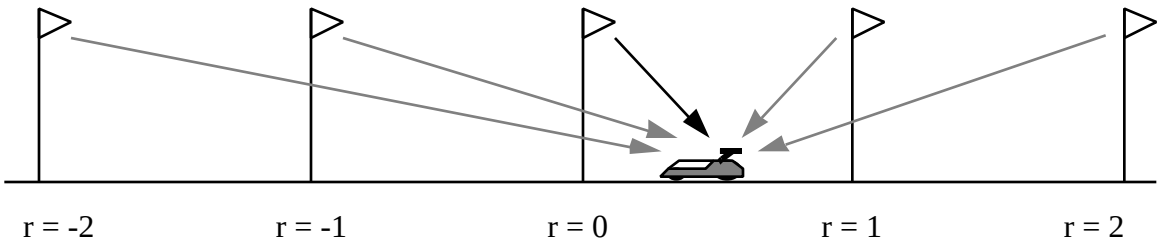

Figure 5.1 Model of base station to vehicle link for frequency reuse distance of one.

5.2 Transmission Considerations

5.2.1 Some Channel Parameters

Similar to the model developed in the preceding chapter, we assume that in a dispersive Rician fading channel, the received signal at the vehicle is in the form of eq. (5) in Chapter 4. The effect of a strong ground reflection is not modelled explicitly. Our motivations here is that beyond a certain turnover distance of a few hundred meters, propagation may well be approximated by a path loss law of the form a proposed by Harley and used earlier in this report. Some fades may occur because of wave cancellation of the line-of-sight and a (ground) reflection near the base station, but these effects do not substantially affect the coverage of cells or the handover process that takes place at cell boundaries.

We model the (delayed) scattered waves in two ways: early reflections with delays much less than the symbol duration. These scatters lead to Rician fading of the wanted signal. Measurements have indicated that for channels comparable to the short range channel addressed here, the Rician K factor may vary from 4 to 1000 (6 to 30 dB) [7]. From Bultitude and Bedal [8], we know that $K = 7$ dB ($K \approx 5$) is reasonable for most micro-cellular channels. In agreement with [5], computations in this report assume $K_1 = 10$ (or 10 dB), where K_1 represents the Rician factor for early scatters.

On the other hand, late reflections cause intersymbol interference, which we approximate as a Gaussian source of interference, of power $1/K_2$ relative to the dominant line-of-sight. If we consider the excessively delayed components to have an exponentially distributed power delay profile with mean value of about $T_{rms} \sim 800$ ns, we find K_2 to be on the order of 1.4×10^7. This delay spread is a somewhat high estimate for some microcellular networks in an urban environment [9], so it presumably also overestimates channel dispersion in a highway propagation environment. As delay spread is modeled to cause Intersymbol Interference, our results tend to be on the pessimistic side. We'll show that its effect is nonetheless small.

For interfering signals, the propagation distance is significantly larger, and because of the relatively low antenna height, a line-of-sight component may not be present. In such cases, Rayleigh fading appears to be a reasonable model.

5.2.2 Probability of Packet Erasure

A packet erasure occurs when errors occur in excess of the correcting capabilities of error correction coding (assuming it is employed). Similar to Chapter 4, 'slow' and 'fast' Rayleigh fading of the wanted signal are considered using the same conditional expressions of bit errors.

5.2.2.1 Fast Fading

With fast fading, the duration of the packets is substantially longer than the time constants of the multipath fading. Further, we assume that during one bit time, the channel characteristics do not change. During reception of a packet, each signal is expected to experience several fades. If it can be assumed that the received amplitude and phase of all signals are statistically independent from bit to bit even though the receiver remains perfectly locked to the wanted signal, the probability of undetected packet errors for BPSK is as in eq. (15) in Chapter 4.

5.2.2.2 Slow Fading

For packets of sufficiently short duration, the received amplitude and carrier phase may be assumed to be constant throughout the duration of the packet. This condition is satisfied if the motion of the mobile terminal during the transmission time of a block of bits is negligible compare to the wavelength. The probability of packet erasure in a block of L bits with M bit error correction is as in eq. (16) in Chapter 4.

The interference power is the sum of powers from individual interfering base stations, found from the large scale path loss equation and using the appropriate distances and

antenna gain factors. In a spatially uniform network with identical base station traffic loads and discontinuous transmission, the transmitter utilization $P(busy)$, i.e., the probability that its packet queue is nonempty, is equal to $P(on)$, the probability that a station's transmitter is switched on. If on the other hand a station transmits continuously even with an empty packet buffer, then $P(on) = 1$. Given the interferer locations or local mean received interference powers, the joint local mean interference power $\bar{p}_t$ becomes a discrete random variable because of random message traffic loads. The probability of successful reception (event S) at distance r from the test base station becomes:

$$P(S|r) = \sum_{\{\bar{p}_t\}} P(\bar{p}_t) \int_0^\infty f_p(p|\bar{p})\, P\langle S|p, \bar{p}_t\rangle dp \tag{1}$$

where we averaged over all possible values of $\bar{p}_t$ and we relate the local-mean power $\bar{p}$ of the wanted signal to the location r. We consider the four nearest co-channel base stations as the most significant sources of interference. (See Fig. 5.1) Numerical results were obtained for the local-mean packet erasure rates with no error correction ($M = 0$). If the interferers are always on, then we have:

$$Q(r) = P(S|r, on) = \int_0^\infty f_p(p|\bar{p})\, P\langle S|p, \bar{p}_t\rangle dp \quad . \tag{2}$$

The interfering sample is assumed to be Gaussian distributed with mean $\bar{p}_t$. Moreover, interference samples between successive bits are assumed to be statistically independent.

5.2.2.3 Numerical Results

Figures 5.2 and 5.3 show results for bit error rates as a function of the Signal-to-Interference Ratio (SIR) for different (average) Signal-to-Noise Ratios (SNR). The bit error rates are clearly rather sensitive to the value of K_1 which hence must be modelled appropriately. Figure 5.2 indicates that the first resolvable reflection and the excessively delayed component

(their relative powers indicated by K_1 and K_2 respectively) are the limiting factors in a noiseless channel. In Fig. 5.3, the average ratio E_b/N_0 is taken to be 17 dB where E_b is the energy per bit, and N_0 is the one-sided spectral density of the noise. This choice of SNR was made to ensure that channel not be rendered unreasonably unreliable for AVCS purposes while at the same time not being unrealistically high. With a SNR of 17 dB, the bit error rates are of course generally higher than the noiseless case, but still acceptable in practical situations. Further, the bit error rates are less responsive to changes in SIRs above 30 dB because the system is limited by the Gaussian noise. The lowest bit error rate achievable as the Signal-to-Interference ratio diminishes in the noiseless case is over 1/10 times that when the SNR is 17 dB. The system is as such noise limited for reasonable SNRs.

In Fig. 5.4, the packet error rates for packets of 200 bits are calculated assuming slow fading and a SNR of 17 dB. This is a reasonable assumption, at 80 kbps and vehicle speeds of 65 miles/hour (11.3 m/sec), where a packet is transmitted during 6 cm of motion.

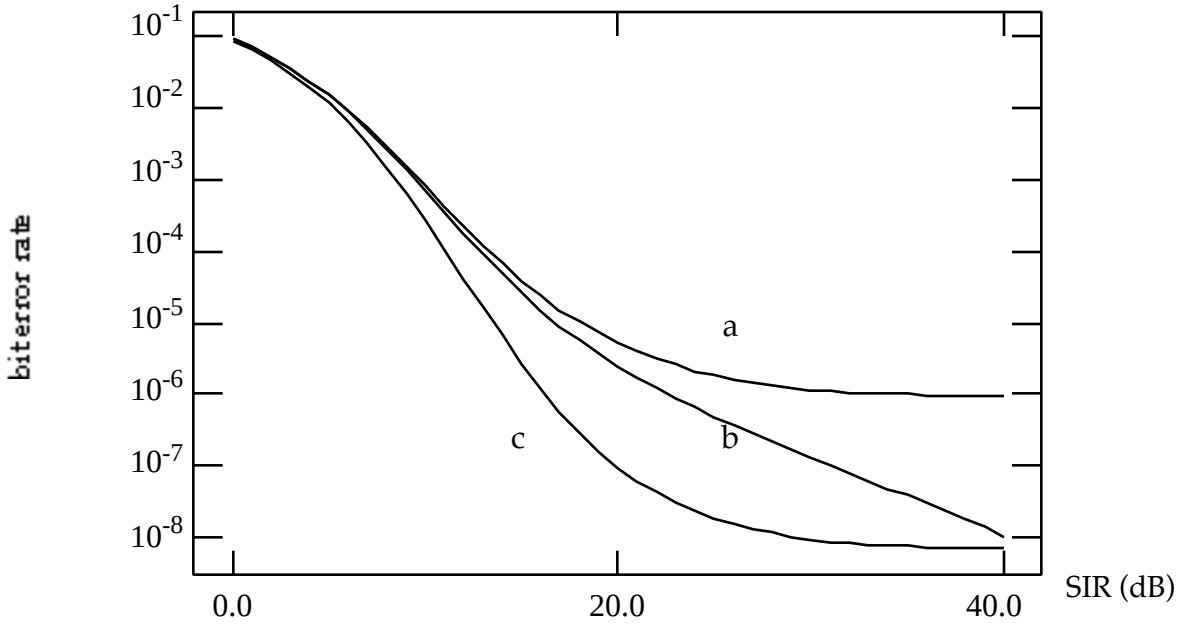

Figure 5.2 Local-mean bit error rates vs. signal-to interference ratio (noiseless channel): (a) $K_1 = 10$, $K_2 = 1.4 \times 10^7$; (b) $K_1 = 10$, $K_2 =$ infinite; (c) $K_1 = 16$, $K_2 = 1.4 \times 10^7$.

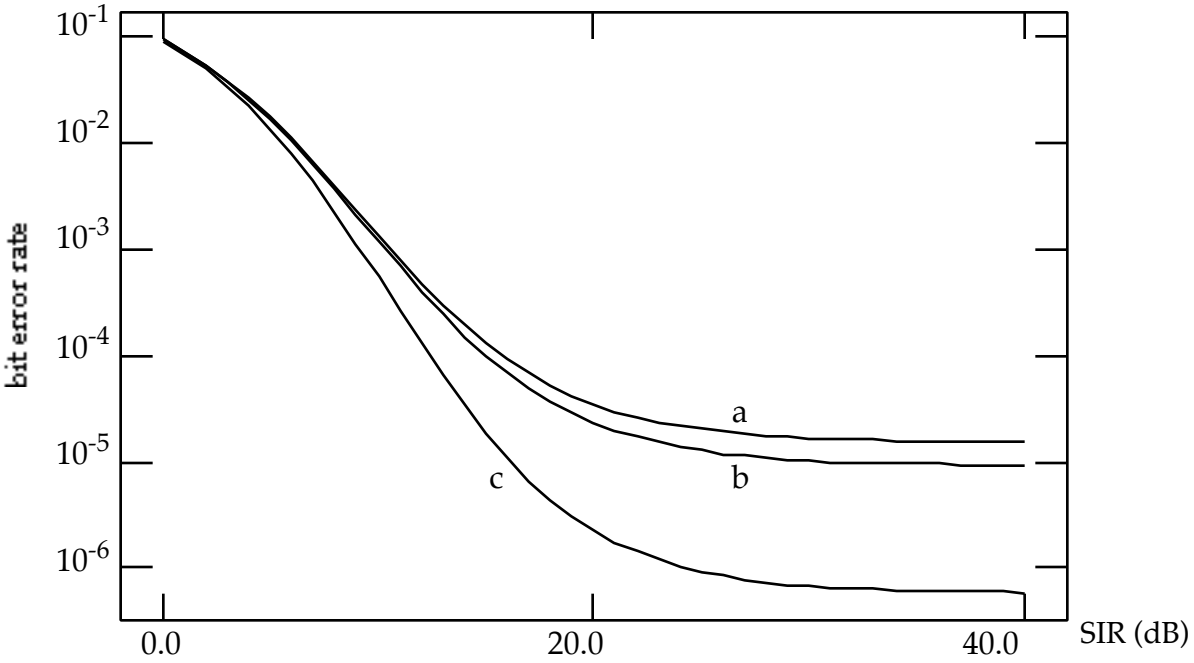

Figure 5.3 Local-mean bit error rates vs. signal-to interference ratio (17 dB SNR) (a) K_1 = 10, K_2 = 1.4 x 10^7; (b) K_1 = 10, K_2 = infinite; (c) K_1 = 16, K_2 = 1.4 x 10^7.

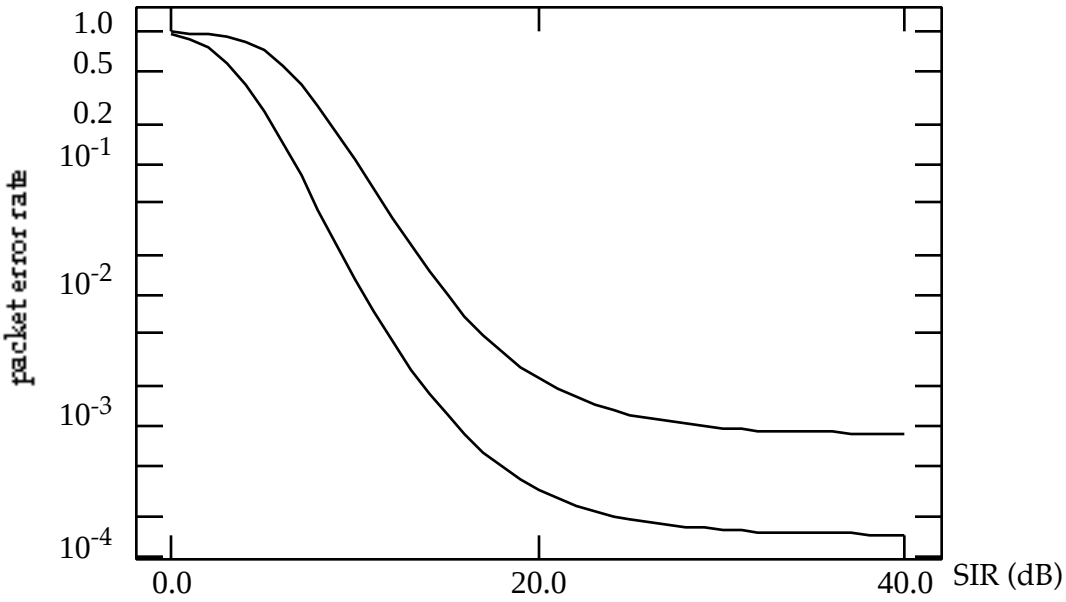

Figure 5.4 Packet error rate vs. signal-to interference ratio (K_1 = 10, K_2 = 1.4 x 10^7, 17 dB

SNR, 200 bit packets): (a) no error correction, (b) 4 bit error correction.

5.3 SPECTRUM EFFICIENCY

In this section, we address the performance of the base station-to-vehicle link in terms of the number of vehicle terminals that may be serviced per unit area, and the delay involved in servicing vehicles.

5.3.1 Packet Erasure Rates as a Function of Distance

The packet erasure rate has been assessed as a function of distance. Fig. 5.5 shows the results of the computation for cluster sizes (frequency reuse distances) of 1, 2, and 3 respectively. The distance between base stations has been normalized to 1, and the reference base station is at 0. Omnidirectional antennae are assumed, and (large scale signal attenuation) eq. (1) in Chapter 3 is used with path loss turnover distance $r_g = 0.25$ to compute the Signal-to-Interference ratio. The case of cluster size 1 shows a packet erasure probability close to unity at the halfway point between base stations. A reuse distance of 2 will yield packet erasure rates of about 0.007 at the cell edge. With a reuse distance of 3, packet erasure rates are very low: just over 10^{-3} at the cell edge (r=0.5) and about 0.1 at the position of the next base station (r=1.0).

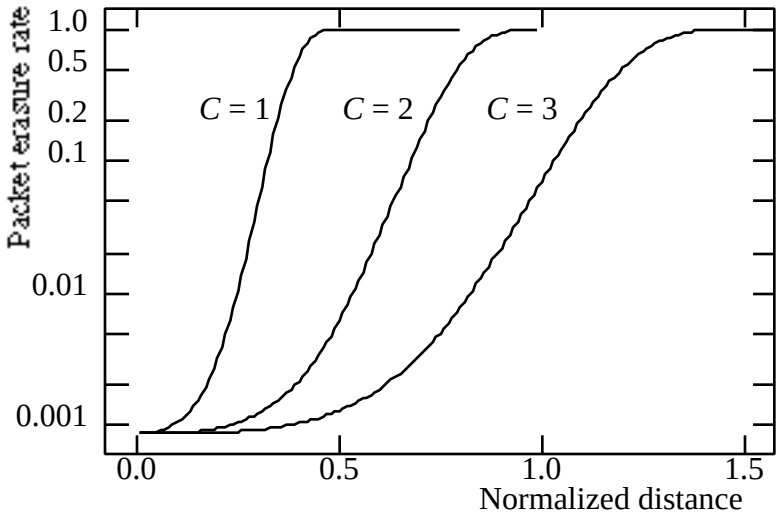

Figure 5.5 Packet erasure rate versus normalized distance from transmitting station. Distance between adjacent stations = 1, omnidirectional antennas, 200 bit packets, no error correction.

5.3.2 Directional Antennas

By using directional antennae at the base stations, reception at the vehicles may be enhanced. End fire arrays or simple metal reflectors may be used to create directivity in the antenna beam. The advantages of directional antennas are due to increased backward attenuation and improved cell confinement.

Directional antennas decrease the amount of co-channel interfering energy because it attenuates propagation to sections of the highway that are behind the antenna. Other studies have also shown that there is a greater confinement of energy in the forward direction on the highway when directionality is introduced to the transmitting antenna [5]. We will investigate the advantages of antenna directionality.

Figures 5.6 shows the erasure rates for transmission of packets with directional antennas having a backward attenuation of 10 dB. The plots are for frequency reuse distances of 3. Our results (e.g. in Fig. 5.6) indicate that there is still a sizeable portion of the cell for which packet transmission is very unreliable for a frequency reuse distance of 1 as was observed in the omnidirectional case.

Ideally, in the omni-directional case, a hand-over should occur at $r = 0.5$. For diectional antennas with a three cell reuse pattern, in order to achieve channel reliability, Fig. 5.6 reveals that the optimum hand-over should take place at about $r = 0.8$. The packet erasure rate at this position is then comparable to that at $r = 0.5$ in the omnidirectional case with three cell reuse. The directionality of the antenna as such seems only to shift the hand-over point without making a significant difference in cell average packet erasure rates. It is seems worthwhile to have directional antennae only if the backward attenuation is reasonably high (higher than 10 dB). The goal should be attenuating interference such that the packet

erasure rate approaches the limit due to the noise floor as in Fig. 5.4 (about 25 dB attenuation).

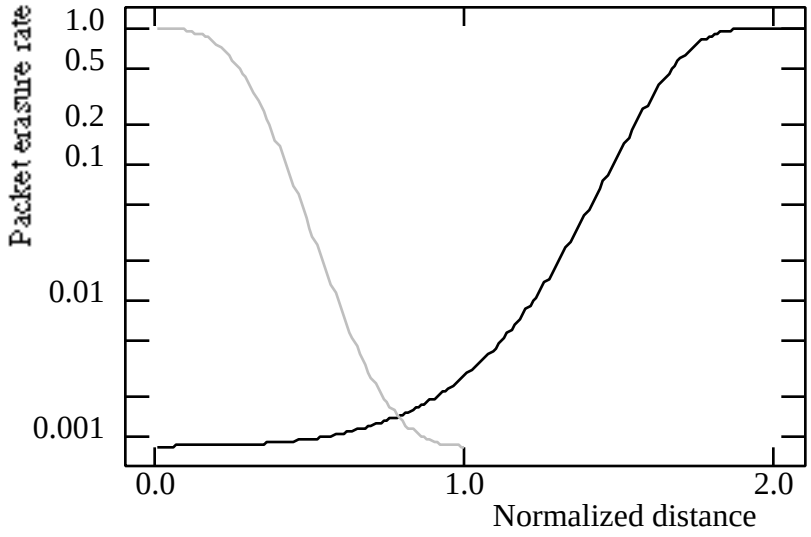

Figure 5.6 Packet erasure rate versus normalized distance from directional transmitter with 10 dB back attenuation for reuse distance of 3.

Fig. 5.7 shows packet erasure rates for a directional antenna with 25 dB back attenuation and for a frequency reuse distance of 1. One interferer is facing the opposing direction, and its power is attenuated by 25 dB. This station still appears to cause unreliability in transmission when the cluster size is 1, even with directional antennae. In Fig. 5.8 we see packet erasure rates for a frequency reuse pattern of 2. There is a slight improvement in cell average packet erasure rates. We conclude that the advantage of directionality is small, Omnidirectional antennae will be assumed in most subsequent computations

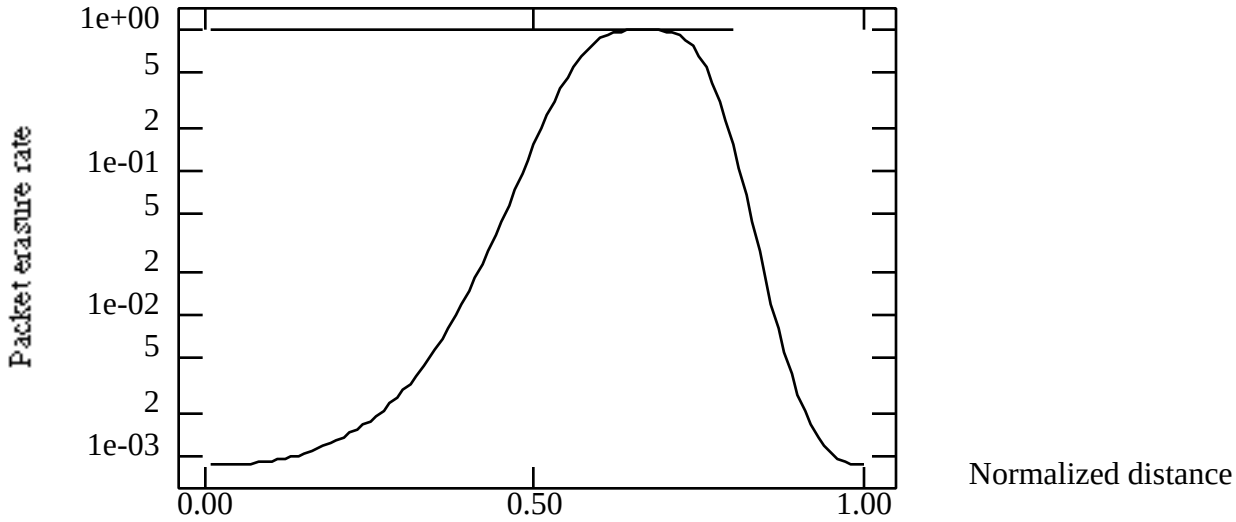

Figure 5.7 Packet erasure rate versus normalized distance from directional transmitter with 25 dB back attenuation for reuse distance of 1.

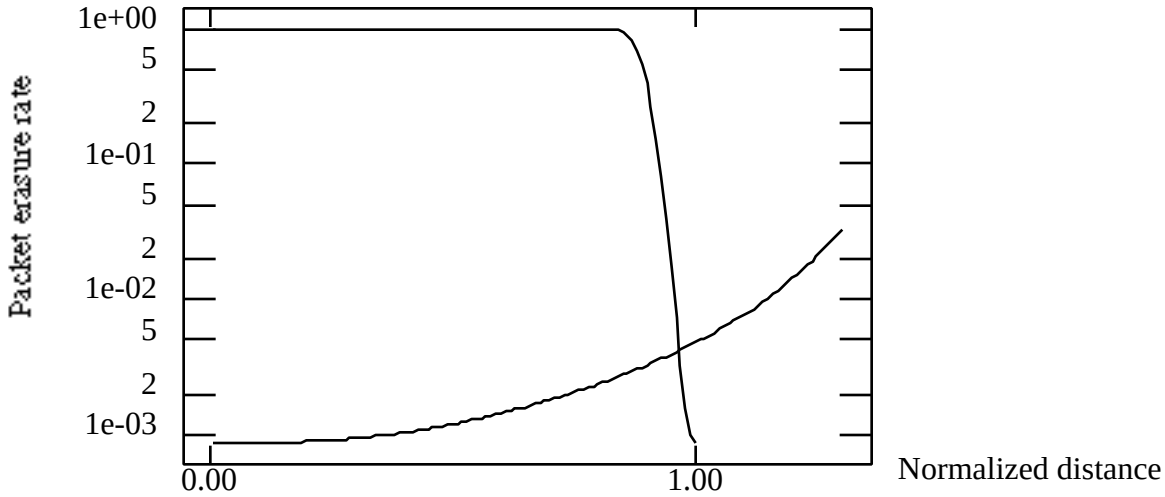

Figure 5.8 Packet erasure rate versus normalized distance from directional transmitter with 25 dB back attenuation for reuse distance of 2.

Another important inference can be made from results on erasure rates. They indicate that if packet retransmissions are used as an indication of a vehicle or platoon's position relative to base stations, hand-overs will be made fairly late. In the case when a reuse factor of

2 is used, hand-overs will be made at normalized distances 0.2 and 1.2 for example, if the maximum allowable average number of retransmissions is 2. This result is for 10 dB back attenuation on the directional antenna. If the directionality is increased, the hand-over points will be further skewed relative to the base stations. The drawback is that the system will not take full advantage of the lower packet error rates resulting from antenna directionality.

5.3.3 Choosing a Reuse Pattern

There are three issues to consider in choosing a reuse pattern. The reliability of the channel is a very important consideration: it would be ideal not to have too many retransmissions of packets. Another important factor is the number of vehicle terminals that can be served per unit cell per unit time. Transmitting at full bandwidth obviously would be optimum if the number of serviced customers per unit time were the only issue. It has however been shown that interference causes unreliability if all stations transmit at full bandwidth. Even with a highly directional antenna, interference will cause many packet erasures when the cluster size is 1. Transmitting at the full bandwidth in every cell hence requires a more innovative approach. This issue will be dealt with later in the chapter.

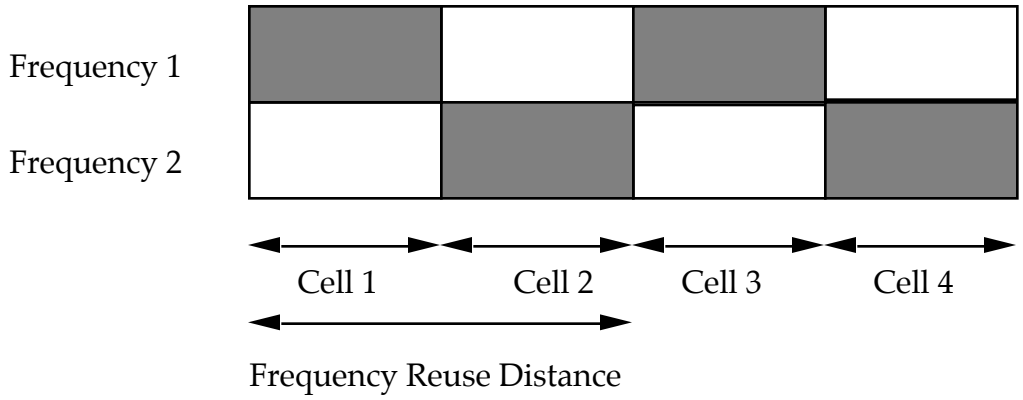

Figure 5.9 A frequency reuse pattern of 2.

Finally, correct hand-over decisions are an issue. A hand-over should be made at the right point and to the right base station. The local-mean number of retransmissions of packets may be used as an indication of whether a hand-over is necessary.

Figs. 5.6 and other computations not reproduced here indicate that based on reliability considerations, a frequency reuse factor of 2 or 3 is much more reasonable than a reuse factor of 1. The plots however, assume that the interfering base stations are always on. This is a rather conservative assumption, but it indicates that by dividing the bandwidth into 2 as demonstrated in Fig. 5.9, we get a much more reliable channel. It also demonstrates that the additional gain from splitting the total bandwidth into 3 frequency bands is not as significant. It can be concluded based on channel reliability, that a frequency reuse pattern of 2 is the reasonable choice. This is more reliable than a reuse pattern of 1, and in both cases of frequency reuse factor of 2 and 3, the average number of packet transmissions required per message is close to 1.

5.3.4 Maximizing Performance

So far, our analyses suggests that a cluster size of 2, using omnidirectional antennas is sufficient. In this section we study the delays that occur due to retransmissions and queueing in the base station. Ultimately, the goal is to minimize the delay, while utilizing the available spectrum efficiently. By delay we mean the total of the wait until service, and the service time for a packet. The following analysis will reveal that denser reuse is favourable.

Vehicle traffic is assumed uniform throughout the cell. It would hence be reasonable to model uniform throughput per unit of area throughout the cell. This assumption however differs from assuming a constant attempted packet traffic to all areas, because areas will poor coverage need more retransmission attempts. The successful total throughput per station is denoted as S_0 $(0 \le S_0 \le 1)$ and represents the number of packets per cell per slot that

are successfully transmitted. For a cluster size of C (the total allocated bandwidth is shared by C cells), we define the spectrum efficiency (spatial packet throughput density) as

$$SE = \eta_r \frac{S_0}{C} \tag{3}$$

expressed in gross user bits per base station per Hz per second. The bit rate per second per Hertz is denoted as η_r. The normalized spectrum efficiency is found from $\eta_r = 1$ bit/sec/Hz.

We will assume that the fading is independent from one transmission to the next, but that the large scale attenuation remains constant during the retransmission delay time. Since the probability of successful packet reception at a given distance $P(S|r)$ decreases with increasing propagation distance r, the expected number of transmission attempts $M(r)$ increases with increasing r.

The delay $D(r)$ is mainly determined by the queueing of packets in the base station: packets with nearby destinations may have to wait because of the transmission time for packets to remote destinations. The delay is less sensitive to r than $M(r)$. The following analysis will therefore address the cell-average delays.

The number of packets waiting in the base station is modelled as a Discrete Time M/G/1/∞ queue. The mean service time $E[\lambda]$ is

$$E[\lambda] = E[E[\lambda|r]] = \frac{1}{R}\int_R \frac{1}{P(S|r)} dr \tag{4}$$

expressed in slots, where the slot time depends on C, and R is the cell size. Once again we have assumed that the distribution of vehicles within the cell is uniform. The cell throughput is found from

$$S_0 = \frac{P(S)}{E[\lambda]} = P(busy)\left(\frac{1}{R}\int_R \frac{1}{P(S|r)} dr\right)^{-1} \tag{5}$$

where $P(busy)$ is the probability that the reference station is transmitting vehicle terminal data. It is equal to the probability that the interfering station is transmitting. Also, since we have assumed uniform throughput rather than uniform attempted traffic, then $P(S) \neq \frac{1}{R}\int_R P(S|r)\,dr$.

Similarly, the second moment of the service time is

$$\mathrm{E}[\lambda^2] = \frac{1}{R}\int_R \frac{2 - P(S|r)}{[P(S|r)]^2} dr \tag{6}$$

The number of packets waiting in a station is modeled as a M/G/1/∞ queue. Assuming immediate retransmissions but nonetheless with independent success probabilities $P(S|r)$, the average delay (using the Pollacek-Khintchine formula) is

$$\mathrm{E}[D] = \left(\frac{LC}{\eta_r B_N}\right)\left[\frac{S_0 \cdot \mathrm{E}[\lambda^2]}{2(1 - P(busy))} + \mathrm{E}[\lambda]\right] \tag{7}$$

The results in Figure 5.10 (normalized to $\eta_r B_N / L = 1$) were computed by letting $P(busy)$ vary from 0 to 1 and getting throughput and delay from the above expression. For any required throughput, delays are less for $C = 2$ than for $C = 3$. At low throughput, C=1 has the least delay, and the delay is inversely proportional to the bandwidth per base station: interference is so low that very few packets need to be retransmitted and delays are close to one packet transmission time. For higher throughput, hence more interference, the delay for $C = 2$ remains less than for $C = 3$ despite the fact that more collisions occur; the delay for $C = 1$ is worse due to many (immediate) retransmissions. A frequency reuse pattern of 2 minimizes delay at high throughput. At low throughput, $C = 1$ has less delay. As we will report in the next sections, it may be possible to further enhance the spectrum efficiency by using $C = 1$ with an efficient 'collision resolution' algorithm to mitigate the effect

of conflicting base station transmissions. This particularly improves the loss of throughput at high offered traffic loads.

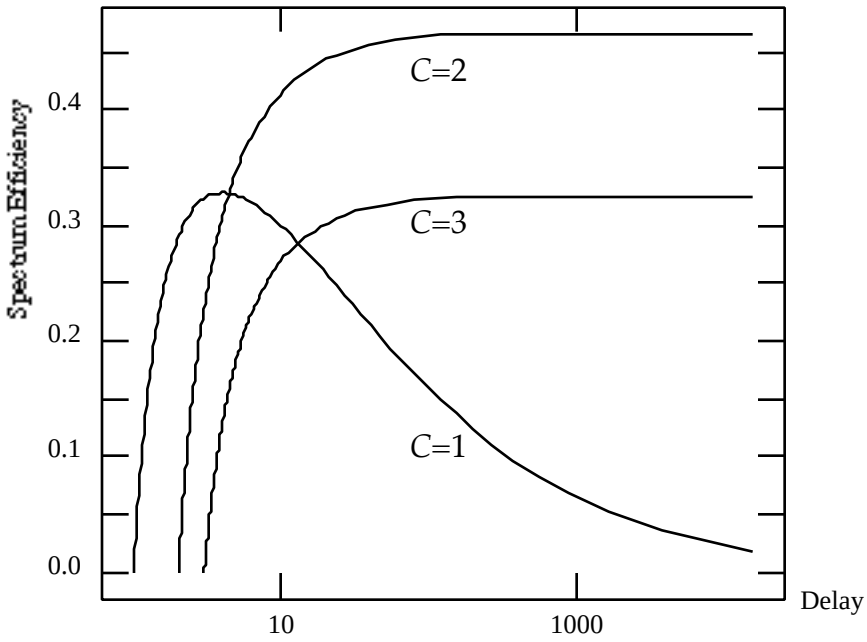

Figure 5.10 Spectrum efficiency and delay for different cluster sizes. ($r_g = 0.25$, $K_1 = 10$, $K_2 = 1.4 \times 10^7$, SNR = 9 dB at cell boundary, 200 bits/packet, no error correction).

The "number of spectrum resources" that a packet consumes on average for successful transmission is $C/Q(r)$ (Fig. 5.11). Near the base station, very few transmissions are needed. Farther away, more are required especially for $C = 1$. The results show that, as r varies, the minimum value for $C/Q(r)$ changes between parameter values of C. This leads us to propose a dynamic cluster size which depends on the location of target vehicles within a cell; i.e., if a vehicle is known to be close to the base station, then it receives downlink packets using $C = 1$. Vehicles which are farther away will receive downlink packets at $C = 2$ or even $C = 3$ to minimize the "number of spectrum resources" used. If this dynamic cluster size method is used, then the expected service time becomes

$$E[\lambda] = \frac{L}{\eta_r R B_N} \int_R \min_C \frac{C}{Q(r)} \, dr \tag{8}$$

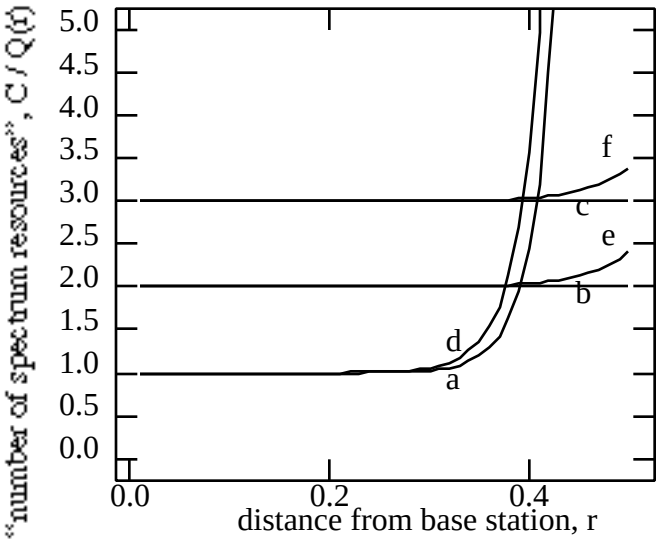

Figure 5.11 "Number of spectrum resources" versus position in cell. (continuously transmitting base stations) No noise: a) *C*=1, b) *C*=2, c) *C*=3; with noise: d) *C*=1, e) *C*=2, f) *C*=3.

The spectrum efficiencies for fixed (*C*=1,2,3) and dynamic cluster sizes were calculated and the results are shown in Table 1. The spectrum efficiency for $C = 1$ is close to zero due to excessive retransmissions to vehicles at the cell boundary. For other values of *C*, the spectrum efficiency approaches the theoretical maximum ($1/C$). For the fixed system, $C = 2$ gives the best spectrum efficiency, but the dynamic scheme gives even better results. Smaller SNR will diminish *SE*.

Extending, if we use perfectly directed antennas (radiating in one direction only so the cell area is $0 < r < 1$ with the base station at the edge $r = 0$), then the spectrum efficiency is increased and we observe that $C = 1$ is optimum. (See Fig. 5.10)

Cluster Size	SNR = infinity	SNR = 9 dB
C=1	0.020517	0.007107
C=2	0.499960	0.490237
C=3	0.333332	0.329033
Dynamic	0.784922	0.742079

Table 5.1 Spectrum Efficiency (continuously transmitting base stations); SNR specified

at cell boundary ($r = 0.5$)

5.3.5 Spatial Collision Resolution

The calculations performed above have assumed that queues contents at adjacent base stations are independent. This is however also not necessarily true. Firstly, if a message intended for a certain vehicle is not transmitted while it is in the cell, it will have to be added to the queue of the adjacent base station. Secondly, packet transmissions at both base stations cause mutual interference which directly affects the lengths of both queues. Nonetheless, independent service times for packets queued at the same base station have been assumed. Therefore, the previous results may be inaccurate under certain conditions. However, transmissions of base stations may be coordinated to avoid the problem of continued mutual interference.

Performance analyses of 'spatial resolution schemes' to resolve collisions in adjacent cells are being performed [22], [23]. In one such scheme all base stations share the same transmit channel which has frames of four time slots. The sections of the highway cover by each base station are assigned a sequence number {1 or 2} according to map-coloring scheme which assures adjacent areas always have a different number. During normal operation, each station may transmit during anytime slot. With some probability a collision occurs, and the interfering power is to strong to allow successful receiver capture. In this case the station will retransmit in its assigned slot while all adjacent stations are silenced. This coordination is performed by sending instructions through the fixed backbone infrastructure connecting all base stations. With this algorithm implemented to resolve the interference problem, it will be possible for all stations to transmit at the full bandwidth with hence high spectral efficiencies and minimal delays.

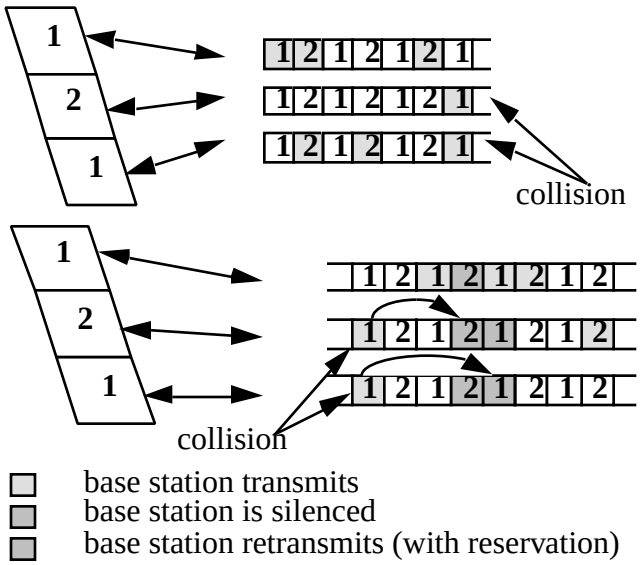

Figure 5.12 Time Slot Usage with Spatial Collision Resolution

To further exploit the benefits of dense frequency reuse, Walrand and Litjens [26] proposed a packet-switched scheme transmitting packets from roadside base stations to vehicles. Arrival processes in the cells are assumed to be homogenuous Poisson processes but with non-identical arrival rates. The proposed scheduling algorithms assign permissions to transmit to the base stations in a conflict-free manner: when a station is activated, its neighbors are silenced, in order to solve the problem of collisions through interference. Both static and dynamic strategies are proposed in [26]. In the former, a fixed broadcast schedule is constructed, describing the time slots in a cycle during which each base station is activated. In the latter, permissions are distributed in each time slot, based on the status (idleness or non-idleness) of all the base stations. A second distinction that is made, is between centralized control, where the network management makes all decisions, and distributed control, where the base stations decide themselves whether or not to transmit, based on the limited information that is exchanged between neighbors.

The proposed algorithm for static strategies with centralized control separates the problem into two parts: (1) the selection of the assignment patterns that are used in the cycle and their frequencies of appearance, and (2) the placement of these patterns in a cycle, aiming to spread the activations as uniformly as possible for each individual base station.

5.4 Uplink Random Access

As the message traffic offered to the uplink is highly bursty, a random access scheme is needed. It was reported in PATH document [27] that it is optimum to use the same inbound frequency in all cells. Next we present some new results on a radio network with two base station receiving packets transmitted by a large population of mobile vehicle terminals. If both stations share the same channel, transmissions in one cell interfere with transmissions in the other cell. Here we discuss a roburst retransmission scheme that avoid instability and migitates the effect of interference between cells. To consider the performance of this two-cell system, we model a one-cell system with time-varying channel properties. If only one station is busy (or if both are silent) the base station is supposed to be in "good state". If both stations are busy the channels are supposed to be in "bad state", due to the mutual interference. Markovian transitions from one state to the other is assumed. For conflict resolution, the stack-algorithm is used [28, 29], which will be explained later on.

Whenever only one base station is busy (or when both stations are silent), this base station is assumed to have a perfect channel (to be in "good state"). When both stations are busy, they interfere, so the channel is imperfect ("bad state"). We approximate these states as Markov transition from one state to the other. The performance of such two-cell system with a common channel (and without any CDMA spreading factor) is compared with the performance of two-cell system with different channels. To avoid the interference in the latter system, 2 different channels would be needed, each with half the bandwidth. That is, the

transmission time increases by a factor two. Moreover the arrival rate of packets per time slot increases by a factor of two. Under large traffic loads, this leads to a significant delay.

5.4.1 Model of Access Scheme

The uplink random access channel is considered to be time slotted and synchronized at time slot level. The slots start at t=1,2,3,... A slot that starts at $t = n$ is called slot n. A packet is transmitted during one slot, and transmission of each packet starts at the beginning of a slot. A new packet is transmitted for the first time in the first slot following packet's arrival (free access). The incoming flow of packets in a cell is a Poisson flow with flow rate λ packets per slot. Each vehicle terminal has a buffer to keep one packet that has to be transmitted. Any packet that captures the receiver leaves the system. Each packet transmitted in a slot without capturing the receiver is either retained in the vehicle terminal's buffer (with probability 1/2) or is retransmitted in the next slot (with probability 1/2). The main idea here is to split the terminals into different smaller groups. the probability of having a message collision in subgroups rapidly vanishes afteer a number of splits. To ensure that each terminal keeps track of the group in which is may transmit, we introduce a stack counter l_n which is associated with the vehicle terminal's buffer and which changes from slot to slot according to the stack-algorithm rules, following the feedback information. Generally, the stack counter increases when a conflict is reported in a slot and decreases when a slot is idle. The idea is that after a collision, all backlogged groups of packets have to wait before the current group has resolved its collision. As the current group splits, a new level is inserted, and all existing groups increase their stack counter.

We address two versions of algorithm [3].

Algorithm A

The algorithm uses ternary "idle slot/success/conflict" feedback.

1a. A packet transmitted in slot n for the first time (i.e. the packet generated in slot n-1) has $l_n = 0$.

2a. If $l_n = 0$ for a packet, the packet is transmitted in slot n. If $l_n > 0$, the packet is not transmitted in slot n.

3a. If $l_n = 0$ for a packet and a conflict is reported in slot n, $l_{n+1} = 1$ with probability $1/2$ and $l_{n+1} = 0$ with probability $1/2$.

4a. If $l_n > 0$ for a packet and a conflict is reported in slot n, $l_{n+1} = l_n + 1$.

5a. If $l_n > 0$ for a packet and slot n is reported idle, $l_{n+1} = l_n - 1$.

6a. If $l_n > 0$ for a packet and a capture is reported in slot n, $l_{n+1} = l_n$.

Rules 1 - 3 address the behaviour of newly arrivaing packets and those that are being (re-) transmitted, while rules 4-6 address backlogged packets.

Algorithm B

The algorithm uses binary "conflict/no conflict" feedback.

1b-5b are the same as 1a-5a, respectively.

6b. If $l_n > 0$ for a packet and a capture is reported in slot n, $l_{n+1} = l_n - 1$.

Thus algorithm B is more aggressive in retransmitting previously collided packets.

The one-cell system can be in two states. If during slot n the system is in state i, i=1,2, then it will stay in the same state during slot $n + 1$ with probability q_i, and will be in different state with probability $(1 - q_i)$. The mean duration of being in state i is equal to $L_i = 1/(1-q_i)$, $i = 1, 2$. The probability for a system to be in state i is $Q_i = L_i/(L_1 + L_2)$, $i = 1, 2$.

Let the system be in state i during a slot n. We model the effect of interference as follows. If the slot n is idle, a capture is reported in this slot with probability z^i_{10}, and a conflict is reported with probability z^i_{0c}. The slot is reported idle with probability $(1- z^i_{01} - z^i_{0c})$. If in the slot n there would be a capture (one packet from that cell was transmitted), a conflict is reported in this slot with probability z^i_1. , and a capture is reported with probability $(1 - z^i_1)$.

If in the slot n there is a conflict, a conflict is reported with probability 1. Thus, in our discussion, we cover interference between cells as errors in the feedback, which would have the same effect.

We assume that the state "1" has a perfect feedback channel, $z^1_{01} = z^1_{0c} = z^i_1 = 0$, and assume that the state "2" has an imperfect feedback channel. For ease of notations, the index "2" is omitted, and the notations are : $z^2_{01} = z_{01} > 0$, $z^2_{0c} = z_{0c} > 0$, $z^2_1 = z_1 > 0$.

The delay of a packet is defined as the length of a time interval between the start of the packet's first transmission and the start of it's successful transmission. Note, that the time a packet spends in the system includes the random waiting time till the beginning of the first transmission, the delay, and one slot of successful transmission. The mean time T a packet spends in the system is equal to the mean delay D plus a slot duration times 3/2.

If the income flow rate $\lambda < \lambda_{cr}$, all packets are transmitted with finite delay with probability 1, and the mean delay finite. The value of λ_{cr} is called the throughput of the system, λ_{cr} depends on the channel probabilities. For given channel probabilitires the mean delay D can be expressed in terms of the solutions of the linear algebraic equations.

The results of computation for one-cell two-state system are compared with the simulation results for two-cell system. In this system both stations use the same stack-algorithm. The performance of two-station system is defined by the following rules.

Let in cell i, i=1,2, slot n be idle. If in cell j with j not equal to i, the slot n is idle too, then in cell i this slot is reported idle. If in cell j there is a capture, then in cell i this slot is reported idle with probability 1 - z_{01} and a capture is reported with probability z_{01}. If in cell j there is a conflict, then in cell i this slot is reported idle with probability 1 - z_{0c} and a conflict is reported with probability z_c.

Let in cell i, i=1, 2, slot n be a capture. If in cell j, with j different from i, slot n is idle, then in cell i this slot is reported to be a capture. If in cell j slot n is not idle, then in cell i a

capture is reported with probability 1- z_1 and a conflict is always correctly reported with probability z_1. A conflict in cell i is always reported to be a conflict in this cell.

5.4.2 Computational Results

To consider the performance of a one-station system we need to introduce the notion of a busy session. Roughly speaking a busy session is a time interval during which there are some packets in the channel, or in the stack of some vehicle terminal, or both in the channel and in the stack. We want to model a two-cell system with the equal income flow rate λ in both cells. Therefore we consider a one-cell two-state system in which the mean length of busy session L_b is equal to the mean length L_2 of the state "2" (i.e. the system being in the "bad state"). The mean length L_1 of the state "1" (i.e. the system being in the "good state") is assumed to be equal to the mean length of the slots without new packets, $L_1 = \frac{1}{1-e^{-\lambda}}$ Therefore $q_1 = e^{-\lambda}$. For given channel properties the value of L_b can be expressed in terms of the solutions of the linear equations (similar to the computations the value of the delay D); q_2 is found by iterations , to satisfy the equality $L_2 = L_b$.

The results of simulations follow the results of computations (for one-cell system) with 10% accuracy.

For the simulation system and for one-cell system C is equal to 1 . The results for one-channel (C = 1) two-state system with income flow rate λ (i.e. for two-cell system using the same channel) are compared with the results for two-cell system with different channels (C = 2).As each channel only has half the bandwidth, time slots need to be twice as large. Effectively, for a given arrival rate per second, this corresponds to a flow rate of twice λ new packets per slot. However, using different channels has the advantage that interference or "feedback errors" do not occur.

The results are illustrated by the tables. In Table 1 we present the mean time T a packet spends in the system and the throughput λ_{cr} for stack-algorithm A. In the Table 2 we present the same data for stack-algorithm B.

In the Tables

a : C=1, $z_{0c} = z_{01} = z_1 = 0$; this system does not suffer any harmful interference between cells.

b : C=1, z_{0c} =1/16, $z_{01} = z_1$ =1/4,

c : C=1, z_{0c} =1/9, $z_{01} = z_1$ =1/3,

d : C=1, z_{0c} =1/4, $z_{01} = z_1$ =1/2,

e : C=2, $z_{0c} = z_{01} = z_1 = 0$. This system uses different inbound channels in the two cells, so mutual interference is absent

f : C=1, $z_{0c} = z_{01} = z_1 = 0$. This system uses only one channel and a single receiving base station covers the two cells.

As in system f no interference from other cells is present, collision resolution can be very efficient. The length of a slot is unity (because of the one cell reuse pattern, the full bandwidth is available in each cell), but the arrival rate per slot is twice the arrival rate in one cell (per slot). So the arrival rates (per slot) in systewm e and f are equal. However, the delays in similar f are half the delays seen in system e. This result is remarkable. It suggests that conventional frequency reuse (system e) is even worse than covering all traffic by a single base station!

System	λ = 0.05	λ = 0.1	λ = 0.15	λ = 0.2	λ_{cr}
a:	0.22	0.60	1.22	2.54	0.33
b:	1.81	2.39	3.84	10.5	0.23
c:	1.87	2.69	7.22	inf	0.16
d:					
e:	4.16	8.08	55.0:	inf	0.16
f:	2.08	4.04	27.5	inf	0.16

Table 5.2 T and λ_{cr} for algorithm A

System	$\lambda = 0.05$	$\lambda = 0.1$	$\lambda = 0.15$	$\lambda = 0.2$	$\lambda = 0.25$	λ_{cr}
a:	0.18	0.47	0.95	1.83	3.79	0.36
b:	1.71	2.06	2.67	3.96	6.77	0.29
c:	1.72	2.09	2.78	4.44	12.29	0.27
d:	1.75	2.19	3.10	7.96	inf	0.2
e:	3.94	6.66	22.69	inf	inf	0.18
f:	2.97	3.33	11.35	inf	inf	0.18

Table 5.3 T and λ_{cr} for algorithm B

Note, that for algorithm B the delay and the throughput do not depend on z_{01}. In the examples the delay is less for the system with $C = 1$, even for relatively large z_{01}.

5.5 Conclusion

An appropriate model for the ITS environment which included a narrowband Rician fading signal with Rayleigh fading interference was proposed. The channel was shown to be slowly fading with the major source of error being co-channel interference. A Rician K parameter of 10 was chosen to model all multipath effects on the highways with a view to computing packet erasure rates. The effect of shadowing was not included in the model. We postulated that during the transmission of a packet and its retransmission, the local mean received power may be considered constant.

It was concluded that error correction coding would not be as efficient as error detection and subsequent retransmission. Also, directional antennas have been investigated to determine the extent to which they increase the efficiency of the network. It was concluded that there is a smallimprovement over omnidirectional antennae, but on the condition that they provide backward attenuation of up to 25 dB. The change in cell average packet erasure rates on the channel is found not to be too significant compared to the omnidirectional case, and so omnidirectional antennas are assumed.

With spatial collision resolution as being investigated in [22], [23], there will be no need for reuse factors of greater than 1. Spectral efficiency and queueing delays would then be optimized. In the absence of such a scheme, it is reasonable to conclude that cluster sizes of 2 are sufficient with the use of directional antennae. This conclusion is based on spectrum efficiency and queueing delay considerations.

For instance, with a frequency reuse pattern of 2 and a bit rate of 80 kbps, an average of 200 successful packet transmissions per second can be achieved, each packet containing about 200 bits. This throughput is more than enough to deal with the cell entry rate estimate of 6 vehicles/second assumed in [19]. The corresponding delay of a few milliseconds per packet suggests that the only limitation on the cell size is the efficiency of the hand-over protocol.

Packet erasure rates have been calculated by averaging over a Rician power distribution. A Rician channel model with a two-ray dominant component has been proposed for the ITS environment. Queues at base stations are modelled as M/G/1, and it is found that, if base stations do not mutually coordinate transmissions, a cluster size C=2 maximizes throughput while minimizing the queueing delay.

Other computations indicate that it is worthwhile to have directional antennas only if the backward attenuation is reasonably high (25 dB), otherwise interference at the cell edge (the vicinity of the interfering station is too high). Hand-overs, based on average numbers of retransmissions, will tend to occur after the vehicle is well into the next cell, and not at the point when the packet erasure rates from both transmitters are equal. The advantage of increased reliability is hence not fully utilized.

Regarding the uplink, our results show that two-cell system with stack-algorithm used for conflict resolution and the same channel used in both cell can be approximated by one-cell system with two states of the feedback channel and with Markov chain transition from one state to the other.

Our results suggest that in future lightly loaded wireless networks with bursty traffic, it may be advantageous to allow near by cells to use the same channels. The free access algorithms appear robust against high levels of interference from co-channel cells. This is in contrast to conventional cellular frequency reuse used for mobile telephones.

5.6 References

[1] K. Takada, Y. Tanaka, A. Igarashi, D. Fujita, "Road/Automobile Communication System and its Economic Effect," *IEEE Vehicle Navigation and Information System Conf.*, pp. A15-21, 1989.

[2] I. Catling and P. Belcher, "Autoguide - Route Guidance in the United Kingdom," *IEEE Vehicle Navigation and Information System Conf.*, pp. 467-473, 1989.

[3] U. Karaaslan, P. Varaiya, and J. Walrand, *Two Proposals to Improve Freeway Traffic Flow,* PATH research report PRR-90-6, Dec. 1990.

[4] H. Harley, "Short distance attenuation measurements at 900 MHz and 1.8 GHz using low antenna heights for microcells", *IEEE J. Sel. Areas in Commun.*, vol. 7, no. 1, 1989, pp. 5-10.

[1] A. Polydoros, et al, "Vehicle to roadside communications study", PATH research report PRR-93-4, June 1993.

[2] J.P.M.G. Linnartz, *Narrowband Land-Mobile Radio Networks*, Boston: Artech House, 1993.

[3] E. Green, "Pathloss and signal variability analysis or microcells", *5th IEE Intl. Conf. on Mobile Radio and Personal Communication*, Warwick, U.K., Dec. 1989, pp. 38-42.

[4] R.J.C. Bultitude and G.K. Bedal, "Propagation characteristics on microcellular urban radio channels at 910 MHz", *IEEE J. Sel. Areas in Commun.*, vol. 7, no. 1, 1989, pp. 31-39.

[5] D.M.J. Devasirvatham, "Radio propagation studies in a small city for universal portable communications", *38th IEEE Vehicular Technology Conf.*, Philadelphia, June 15-17, 1988, pp. 100-104.

[6] J.G. Proakis, *Digital Communications*, 2nd ed., New York: McGraw-Hill, 1989.

[7] R. Ziemer and W. Tranter, *Principles of Communications - Systems, Modulation and Noise*, 3rd ed., Boston: Houghton Mifflin, 1990.

[8] I.M.I. Habbab, M. Kahvehrad and C.E.W. Sundberg, "ALOHA with capture over slow and fast fading channels with coding and diversity," *IEEE J. Sel. Areas in Commun.*, vol. 7, no. 1, Jan. 1989, pp79-88.

[9] K. Zang, K. Pahlavan and R. Ganesh, "Slotted ALOHA networks with PSK modulation in Rayleigh fading channels", *Electron Lett.*, Vol 23, No 6, 16th March 1989, pp. 413-414.

[10] A.J. Jong, "Average bit error rates for coherent detection in macro and micro-cellular radio", *IEE International Conference on Mobile Radio and Personal Communication*, Warwick, Dec. 1991 pp. 241-247.

[11] W.C. Jakes (Ed.), *Microwave Mobile Communication*, New York: Wiley, 1974.

[12] R.E. Blahut, *Theory and Practice of Error Control Codes*, MA: Addison-Wesley, 1983.

[13] S.R. Sachs and P. Varaiya, *A Communication System for the Control of Automated Vehicles*, PATH technical memorandum 93-5, 1993.

[14] D.C. Cox and R.P. Leck, "Distributions of multipath delay spread and average excess delay for 910-MHz urban mobile radio paths", *IEEE Trans.on Antennas and Propagation*, vol. 23, no.3, Mar. 1975, pp. 206-13.

[15] J. Walrand, *An Introduction to Queueing Networks*, Prentice-Hall: New Jersey, 1988.

[16] J.P.M.G. Linnartz, "Contiguous frequency assignment in wireless packet-switched networks", *IEEE Int. Symp.on Personal Indoor and Mobile Radio Communications*, Yokohama, Japan, Sept. 1993.

[17] R. Diesta, Internal research memorandum, U.C. Berkeley

[18] C.O. Eleazu, *A Study of Base Station to Vehicle Communication for Intelligent Vehicle / Highway Systems*, Research Project, EECS Dept, University of California, Berkeley. 1993.

[19] R.F. Diesta, C.O. Eleazu and J.P.M.G. Linnartz, "Packet-switched roadside base station to vehicle communication for Intelligent Vehicle/Highway Systems", *IEEE Veh. Technol. Conf.*, Sweden, June 1994.

[20] R.F. Diesta and J.P.M.G. Linnartz, "Multiple access and spatial collision resolution for IVHS packet radio networks", *IEEE Int. Symp. on Personal, Indoor and Mobile Radio Communications*, The Hague, The Netherlands, Sept. 1994, pp. 1260-1263.

[21] R.F. Diesta and J.P.M.G. Linnartz, "Spatial collision resolution for packet-switched multiple-access wireless networks", *28th Asilomar Conf. on Signals, Systems, & Computers*, Pacific Grove, California, Oct. 1994, pp. 234-237.

[22] R. Litjens, *Conflict-Free Scheduling of Broadcasts in a Linear Packet Radio Network*, Masters Thesis, Dept. of Econometrics, Tilburg University, August 1994.

[23] N.D. Vvedenskaya, "Performance of stack algorithm in case of mutually interfereing transmission in two cells", *Benelux IEEE Symposium on Information Theory*, Noordwijk, Netherlands, May 1995.

[24] N.D. Vvedenskaya and B.S. Tsybakov, "Packet delay with multi-access stack algorithm", *Problems of Information Transmission*, v.16, (1984).

[25] N.D. Vvedenskaya, "Multiple access stack-algorithm with imperfect feedback", *IEEE Int. Symp. on Personal, Indoor and Mobile Radio Communications*, The Hague, The Netherlands, Sept. 1994, pp. 1126-1128.

[26] N.D. Vvedenskaya, J.C. Arnbak and B.S. Tsybakov, "Improved performance of mobile data networks using stack-algorithms and receiver capture", *March 1994 Int. Zurich*

Seminar on Digital Communications, Springer-Verlag, Lecture Notes in Computer Sci., 464-475 (1994).

[27] J.P.M.G. Linnartz and N. D. Vvedenskaya, "Optimal delay and throughput in packet switched CDMA network with collision resolution using stack-algorithm" *Electronics Letters*, 1st Sept., No.18, 1470--1471.

5.7 Appendix A

5.7.1 An Improved Model for Interfering Signals

Section 4.4 described the mean error probability for BPSK modulation with Rayleigh faded co-channel interference. This assumed that interfering signals are perfectly synchronized with the wanted signal. This assumption may be unrealistic. Also, there are likely to be random frequency shifts due to oscillator drifts and random Doppler shifts. In this section we will analyze their effect.

An interfering signal experiences a reversal at $t = (k + \alpha_i) T_b$, where k is an integer, and α_i $(0 < \alpha_i < 1)$ is the synchronization bit offset, normalized to the bit time.

$k_{\leftarrow}$ = bit value for $kT_b < t < (k + \alpha_i) T_b$, and 0 for $(k + \alpha_i) T_b < t < (k + 1) T_b$,

$k_{\rightarrow}$ = 0 for $kT_b < t < (k + \alpha_i) T_b$, and reversed value for $(k + \alpha_i) T_b < t < (k + 1) T_b$

Our received signal is hence

$$r(t) = a_0 \rho_0 \cos(\omega_c t) + \sum_{i=1}^{N} \rho_i \{k_{\leftarrow} \alpha_i + k_{\rightarrow} (1 - \alpha_i)\} \cos(2\pi (f_c - f_i) t + \varphi_i) + n(t) \quad (9)$$

where $n(t)$ denotes Gaussian noise, and the user bits a_0 are +1 or -1. The values of the interfering bits before and after reversal during a bit time denoted $k_{\leftarrow}$ and $k_{\rightarrow}$ are +1 or -1. The instantaneous frequency offset f_i is due to random Doppler shifts and transmit oscillator drifts.

At the receiver the decision variable v is obtained from the correlation operation

$$v = 2\int_0^{T_b} r(t)\cos(\omega_c t)\,dt \ . \tag{10}$$

We then get,

$$v = a_0\rho_0 T_b + \sum_{i=1}^{N}\xi_i\{k \leftarrow \alpha_i + k \rightarrow (1-\alpha_i)\}\int_0^{T_b}\cos(\omega_i t)\,dt$$
$$+ \sum_{i=1}^{N}\zeta_i\{k \leftarrow \alpha_i + k \rightarrow (1-\alpha_i)\}\int_0^{T_b}\sin(\omega_i t)\,dt + N_i \tag{11}$$

where, because of fading, the in-phase component, $\xi_i = \rho_i\cos\varphi_i$, and the quadrature component, $\zeta_i = \rho_i\sin(\varphi_i)$, are Gaussian random variables. Their variances are found as $E(\xi^2) = E(\zeta_i^2) = \bar{p}_i$. Also, $E(n_i^2) = N_0/T_b$.

The conditional variance of the i-th interfering signal is hence

$$2\bar{p}_i(1-2\alpha_i)^2\mathrm{Sinc}(\omega_i T_b) \tag{12}$$

and we therefore have the conditional probability of error:

$$P\langle error|\omega_i, \alpha_i, p_i, \rho_0\rangle = \frac{1}{2}\mathrm{erfc}\left(\sqrt{\frac{\frac{1}{2}\rho_0^2 T_b\mathrm{Sinc}(\omega_i T_b)}{2\sum_{i=1}^{N}\bar{p}_i(1-2\alpha_i)^2\mathrm{Sinc}(\omega_i T_b) + N_0}}\right) \tag{13}$$

We have assumed that oscillator drifts are minimal, and hence we can model ω_i as random FM. Due to the reduced angle of elevation and the typically large distance between the receiver and the co-channel interference transmitters, there is a very high chance that the LOS and ground reflected waves are obstructed by other vehicles on the road, it is likely that the interference is Rayleigh fading. The distribution of ω_i as such can be taken to be

$$f_{\dot{\theta}}(\dot{\theta}) = \frac{1}{2\sqrt{2}}\left(1 + 2\left[\frac{\dot{\theta}}{2\pi f_d}\right]^2\right)^{-3/2} \tag{14}$$

as discussed in [15]. f_d is the maximum Doppler shift. If the base stations are operated independently, the density of α_i is most likely uniform on $0 < \alpha_i < 1$, in which case

$$P\langle error|\bar{p}_i, \rho_0\rangle = \int_0^{\infty}\int_0^{0.5} \frac{1}{2}\mathrm{erfc}\left(\sqrt{\frac{\frac{1}{2}\rho_0^2 T_b}{2\sum_{i=1}^{N}\bar{p}_i(1-2\alpha_i)^2\mathrm{Sinc}(\omega_i T_b) + N_0}}\right) 2f_{\dot{\theta}}(\dot{\theta})\, d\alpha_i d\dot{\theta} \quad . \tag{15}$$

A more accurate analysis, however, would have to take into account the fact that the instantaneous power of the interfering signal and $\dot{\theta}$ may be correlated [15].

If no bit synchronization offset between contending signals is assumed ($\alpha_i \equiv 0$ for i = 1, 2,3,...,n), then conservative results are obtained because it will overestimate the effect of interference. Moreover, in the case of random α_i, the worst-case interfering BPSK bit sequence $k_{\leftarrow} = k_{\rightarrow}$; i.e., no phase reversal is expected to occur during 50% of the bits in the test packet. This event gives the same probability as the case $\alpha_i = 0$. Computations in this chapter assume $\alpha_i = 0$ and $\omega_i = 0$.